

Chapter 1 Introduction

1.1 Background and Motivation

In the field of power electronics, there is a trend for pushing up switching frequencies of switched-mode power supplies to reduce volume and weight. This trend inevitably contributes to an increasing level of electromagnetic interference (EMI) emissions. It leads to a general electromagnetic compatibility (EMC) degradation for electronic devices. As a consequence, EMC legislation is getting more stringent in many countries.

Electromagnetic Interference (EMI) problems in switching power supplies have been traditionally treated with cut-and-try approaches. In recent years, advancement has been made to better understand the problems and minimize the cut-and-try portion of the design process. However, there are still phenomena difficult to explain in many practical design situations. Very often, the problems may be solved by luck but many puzzles remain unsolved.

Conventionally, the total conducted EMI noise is caused by two mechanisms, the differential-mode (DM) and the common-mode (CM) noise. Generally speaking, the DM noise is related to switching current and the CM noise is related to capacitive coupling of switching voltage into line impedance stabilizing network (LISN), which is used in standard conducted EMI measurement. Fig.1-1 shows the typical setup for conducted EMI measurement. The LISN contains inductors, capacitors and 50Ω resistors. For 60 Hz line frequency, the inductors are basically shorted, the capacitors are open, and the power

passes through to supply the equipment under test (EUT). For EMI noise frequency, the inductors are essentially open, the capacitors are shorted and the noise sees 50Ω resistors. The noise voltage measured across the 50Ω input impedance of a spectrum analyzer is defined as the conducted EMI emission.

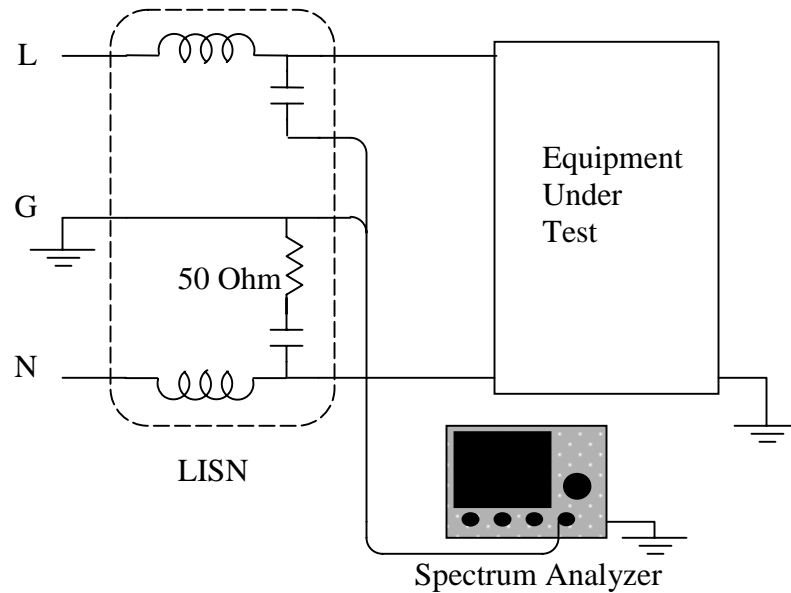


Fig. 1-1 Conducted EMI Measurement Setup

EMI filters are normally divided into two sections, one deals with DM noise and the other deals with CM noise. Usually, both DM and CM noises need to be suppressed to pass EMI limits.

One of the phenomena uncovered recently is the Non-Intrinsic Differential-Mode (NIDM) noise in an off-line switching power supplies [1]. This phenomenon was

accidentally discovered in the process to explain certain EMI filter action but was never thoroughly investigated. The focus of the thesis is to further study the phenomenon and to investigate the implications of this phenomenon to practical EMI filter design issues.

1.2 Outline of Thesis

In the thesis, the NIDM phenomenon will be briefly reviewed in chapter 2, which is crucial to the understanding of the remaining chapters. Two diagnostic tools were used to investigate this phenomenon. One is the DM/CM noise separator [2] and the other is the zero-span mode operation of a spectrum analyzer. Both of these will be reviewed in this chapter.

In chapter 3, the results of the investigation will be presented. The results will be presented using practical examples, which tie the phenomenon to filter design issues. In some examples, explanations are given to dispel the puzzles commonly encountered in the practice.

In view of the NIDM phenomenon, the design procedure for EMI filter needs modification. This is the topic of Chapter 4. A practical filter design procedure presented in [3] will be modified to incorporate the NIDM phenomenon. Only first-order and second-order filter topologies are included in the discussion.

Chapter 5 concludes the thesis with recommendations for future research possibilities.

Chapter 2 Non-Intrinsic Differential Mode Noise

In this chapter, the basic mechanism of Non-Intrinsic Differential Mode conducted EMI emission will be reviewed. A commonly used switching power supply circuit will be used as an example to illustrate the phenomenon. The review of this phenomenon is crucial to the understanding of the remaining chapters of the thesis. Before the NIDM review, a conventional theory of conducted EMI coupling mechanism will also be briefly reviewed.

2.1 Review of Conventional Conducted EMI Theory

Fig.2-1 shows a typical offline switching power supply with conducted EMI measurement setup. In the diagram, a Line Impedance Stabilizing Network (LISN) is used for the measurement of conducted EMI emissions. LISN is used as a standard for repeatable EMI measurement. The standard components inside the LISN are such that for 60 Hz AC power, the inductance ($50\mu\text{H}$) presents very small impedance and capacitor ($0.1\mu\text{F}$) is essentially open circuit. Therefore, the 60Hz power flows unperturbed. For high frequency noise, however, the inductance looks like open circuit and the capacitor is basically short circuit.

Because of the switching nature of the circuit, high frequency noise current could be coupled into the 50Ω resistors. The voltage across the 50Ω resistors is counted as the

conducted EMI emission. Both the line side (V_x) and the neutral side (V_y) EMI must pass specs. The noise is classified into two modes: Common-Mode (CM), which is average of V_x and V_y $((V_x+V_y)/2)$, and Differential-Mode (DM) which is the difference between V_x and V_y (V_x-V_y).

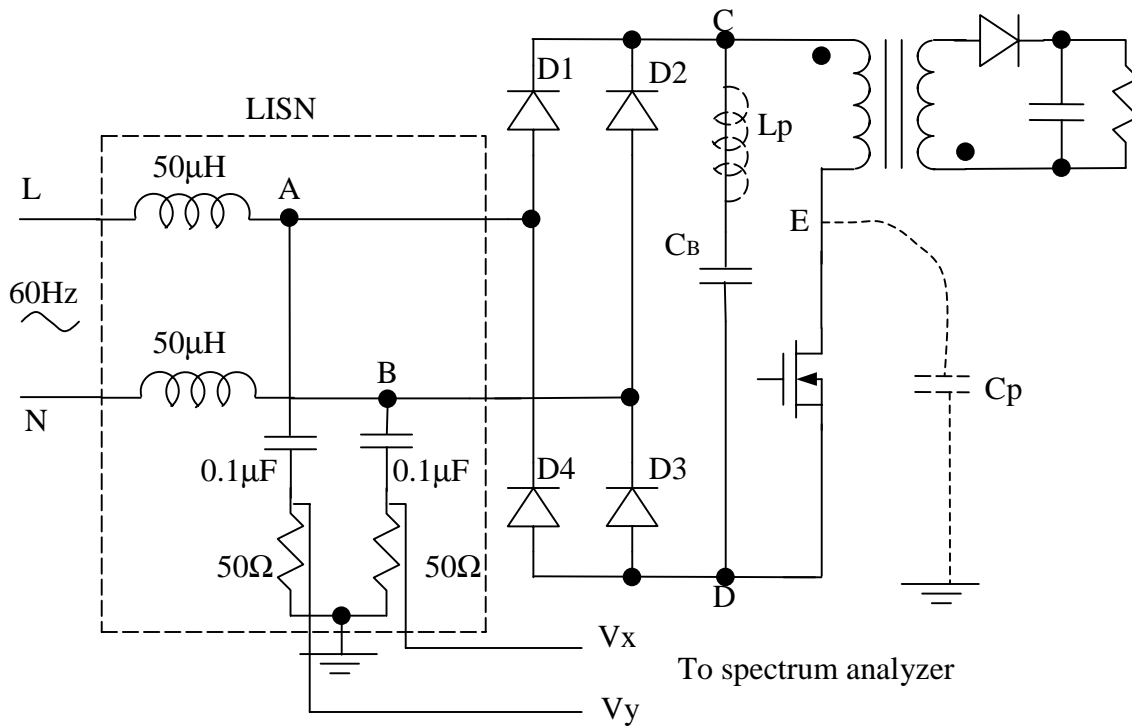


Fig.2-1 A Typical Switching Power Supply Circuit

2.1.1 CM Noise

The CM noise is coupled through C_p , the parasitic capacitance between the drain of the MOSFET (which is usually tied to the heat sink) and the metal enclosure (which is tied to the ground for safety reason) of the power supply. Since the MOSFET is operated as a switch, the drain voltage swings from low to high in half of the switching cycle and from high to low in the second half of the switching cycle. This voltage swing in turn causes the charging and discharging of the parasitic capacitance. The charging and discharging current will return through the ground path and show up on the LISN resistors as CM noise. The CM noise path is illustrated with dash line in Fig.2-2. Notice that the noise current flows through the two 50Ω resistors in parallel.

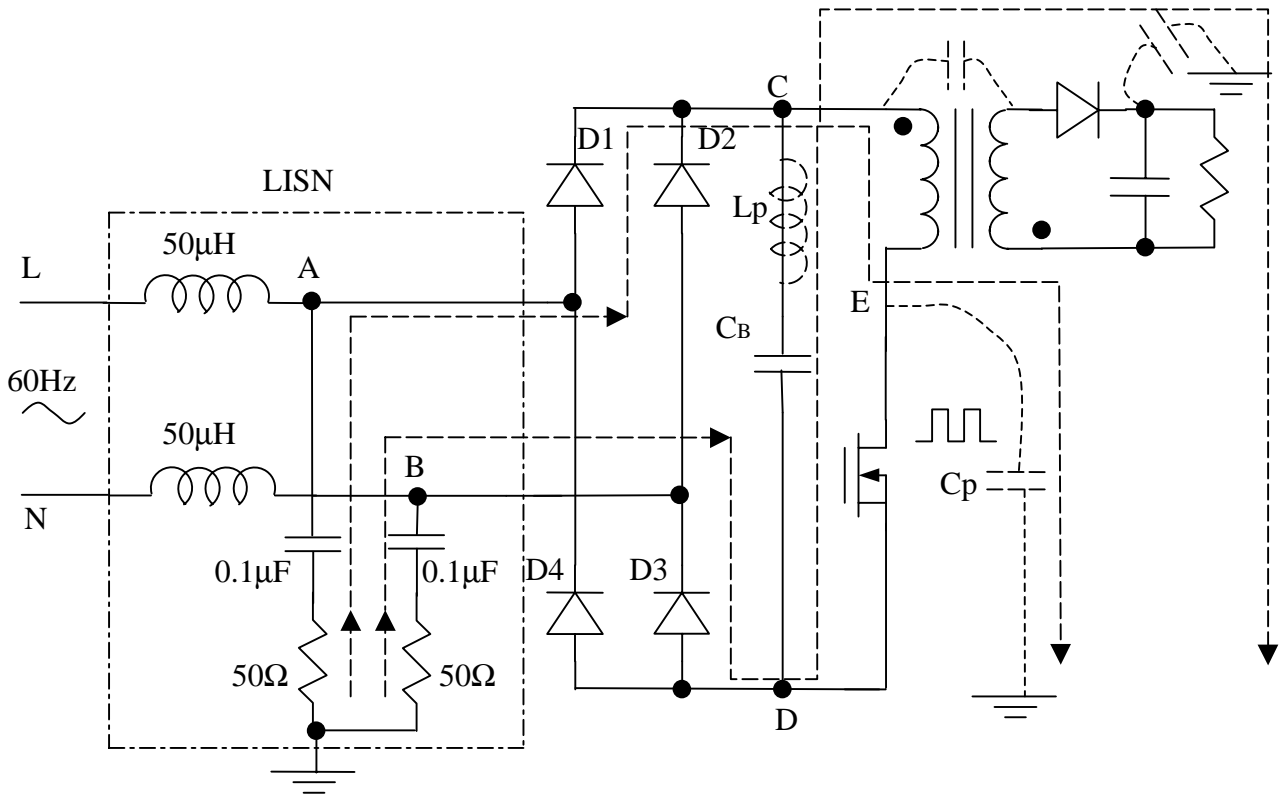


Fig.2-2 Noise Path of CM Noise

Fig.2-2 shows the current path when C_p is charged. When C_p is discharged, the current direction reverses but both currents flow in phase. Therefore, it is called common-mode noise. In general, CM noise is voltage dependent and depends on parasitic capacitance. Besides the parasitic capacitance of MOSFET drain, there are other parasitic capacitors (such as the parasitic capacitance between the transformer primary and secondary windings and the parasitic capacitance of the secondary rectifier diode), through which the CM noise current can couple.

2.1.2 DM Noise

Another mode of conducted EMI noise coupling through the 50Ω resistors is shown in Fig.2-3. Because of the switching nature of the MOSFET current, part of the switch current flows through the bulk capacitor C_B and part through the 50Ω resistors as indicated by the dash line. Since C_B is not perfect due to the existence of parasitic inductance L_p , there is certain amount of noise current flowing through the 50Ω resistors. Notice that the current flows through the resistors in series. In general, the DM noise current is load dependent and is affected by L_p and C_B . This is what the conventional theory says. But in further exploration, we can find there is insufficiency in the theory to explain certain noise phenomenon. A new noise coupling mechanism call Non-Intrinsic Differential Mode (NIDM) noise was uncovered [1] recently. This phenomenon will be discussed in Section 2.3.

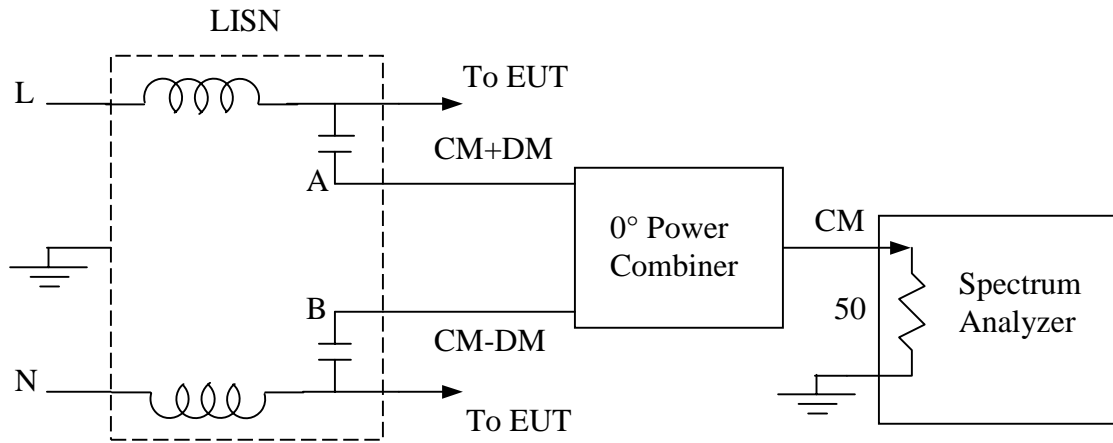
2.2.1 Noise Separator

The noise spectrum measured directly from LISN resistors is total noise. To investigate CM and DM respectively, a noise separator [2] was used for separating CM noise from DM noise.

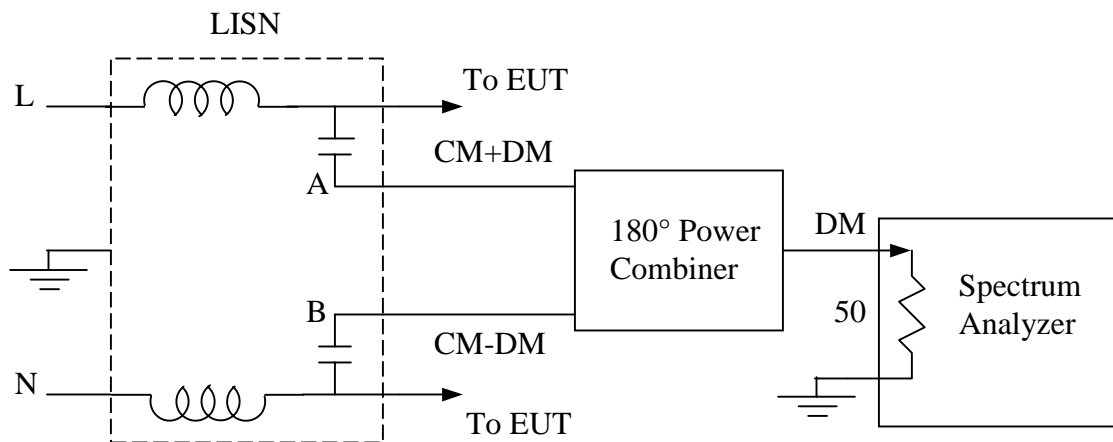
The concept of the noise separator is very simple. Fig.2-4 shows the diagrams depicting this concept. Two signals (A and B) derived from the LISN consist of both CM and DM noises. However, one of the signals is the vector sum of the two modes, and the other signal is the vector difference of the two modes. It is assumed that the CM current is often evenly divided between the two input terminals.

A device called power combiner is used to separate these two kinds of noises. There are two types of power combiners in the noise separator, 0° power combiner and 180° power combiner. The output of a 0° power combiner is the sum of the two input signals, and the output of a 180° power combiner is the difference of the two input signals. In the noise separator, the 0° power combiner cancels out the DM component and lets through the CM component through. The 180° power combiner cancels out the CM component and lets through the DM component.

Power combiners are used mainly for the radio frequency performance because of the EMI frequency requirement. The insertion of the noise separator does not perturb the measurement setup because the impedance seen from point A to ground (or from point B to ground) is still 50Ω .



(a) DM Rejection



(b) CM Rejection

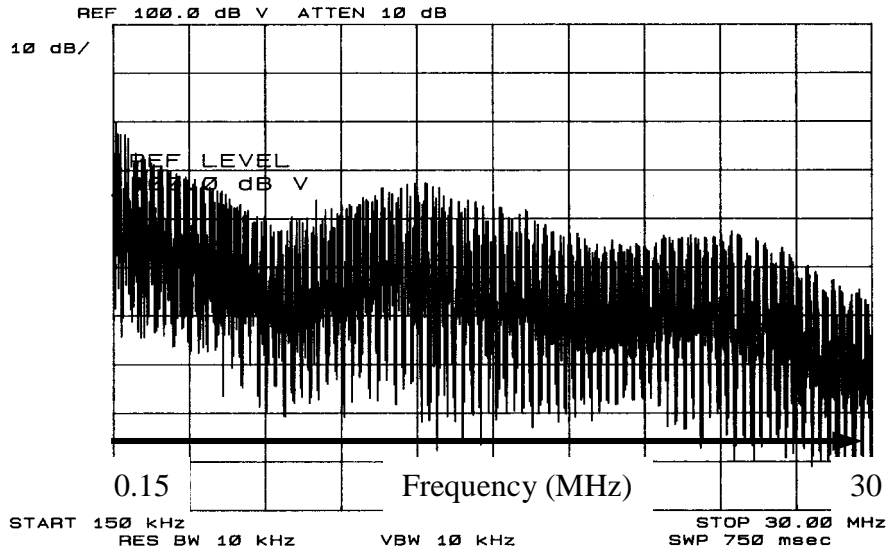
Fig.2-4 Principles of Noise Separator

2.2.2 Zero-Span Mode of Spectrum Analyzer

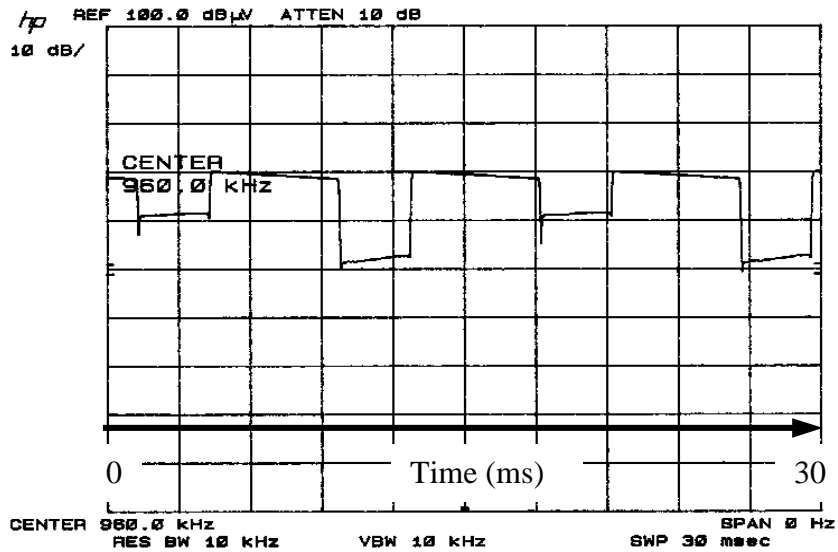
Zero-span mode is a special operation mode of a spectrum analyzer. In this mode, the spectrum analyzer scans at a fixed frequency point (center frequency) and displays the amplitude in term of time. In zero-span mode, the spectrum analyzer behaves just like an oscilloscope; i.e. the horizontal axis represents time instead of frequency. The major difference between a spectrum analyzer in zero-span mode and an oscilloscope is that the spectrum analyzer usually detects and displays only the peak of the time domain signal at the output of RBW filter, while the oscilloscope displays instantaneous values.

Zero-span mode is sometimes a more convenient way to look at amplitude-modulated signals when the modulating signal is of very low frequency.

Fig. 2-5 illustrates two pictures. Fig.2-5 (a) shows the typical EMI noise spectrum. The horizontal axis is the frequency. The emission level, in some cases, may fluctuate with time. In such cases, obviously, the peak of the emission has to pass the specs. If one wishes to investigate the fluctuating behavior of the emission at a particular frequency, then the Zero-Span mode operation of the spectrum analyzer should be used. Fig.2-5 (b) shows the emission at 960kHz in zero-span mode. Notice that the horizontal axis now is the time. In other words, the fluctuating behavior of this frequency is displayed in that picture. This mode of operation will be used frequently in the remaining chapters.



(a) Noise Displayed in Normal Operation Mode



(b) Noise Displayed in Zero-Span Mode

Fig.2-5 Spectrum Analyzer Display of EMI Noise

2.3 Non-Intrinsic Differential Mode Noise

2.3.1 Description of NIDM Phenomenon

Fig.2-6 shows the standard EMI emission measurement results obtained using spectrum analyzer. In the oscillogram, the amplitude of the spectrum fluctuate with time because of input rectifier diodes “on” and “off”. One would ask: “Is the EMI emission larger when the rectifier diodes are ‘on’ or when they are ‘off’?” From the conventional conducted EMI theory given in Section 2.2, one would naturally assume that EMI is larger when diodes are “on”. Because when diodes are “on”, the noisy switch current flows through the 50Ω resistors. However, the experimental results shown in Fig.2-7 indicate otherwise as will be explained below.

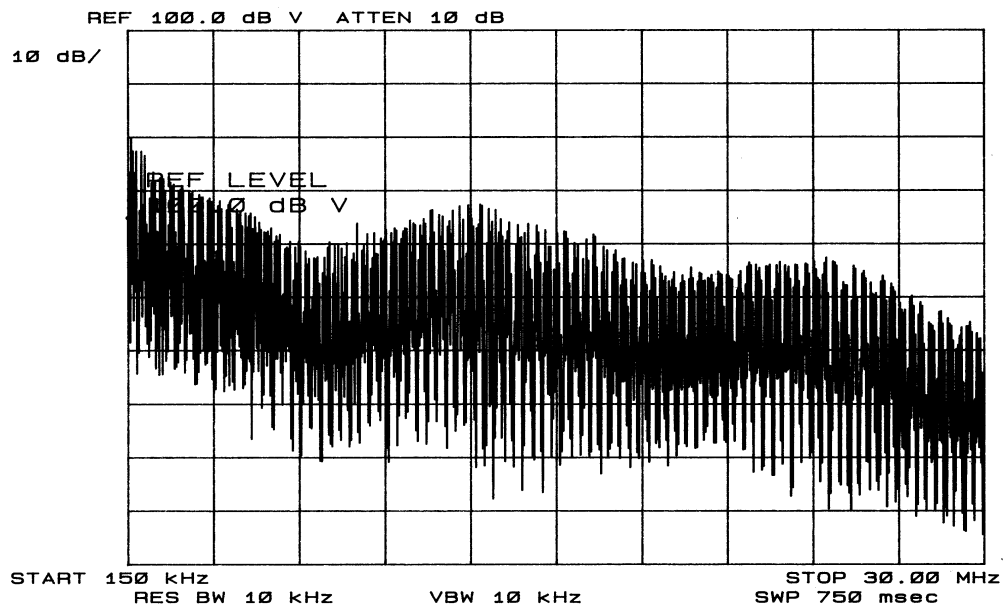


Fig.2-6 DM Emission Measurement Result

Two time intervals are marked in the figure. Interval A corresponds to the “on” state, and interval B to the “off” state of input rectifier diodes. The two intervals together form a complete 120 Hz cycle, which is two times the input line frequency. It can be seen that the noise is higher when the rectifier diodes are cut off than when two diodes are conducting. This phenomenon cannot be explained by conventional theory of DM noise generation. Investigation of that phenomenon led to the discovery of a new DM noise-coupling mode. DM noise coupled through LISN with this phenomenon is called Non-Intrinsic Differential Mode (NIDM) noise. To distinguish, we call the noise coupled through when rectifier diodes are “on” Intrinsic Differential Mode (IDM) noise. The conventional EMI theory can only explain the generation of IDM.

2.3.2 NIDM Noise Generation Mechanism

2.3.2.1. Rectifier Diodes On

First, we consider the situation when two of the rectifier diodes are conducting. Fig.2-8 illustrates the noise current path when the switch is being turned off. When the switch is off, the voltage potential of point E is raised from zero potential to V_2+V_3 . The parasitic capacitance C_p is being charged by V_2 and V_3 . There exist two noise current paths. One path is from the earth ground, passing by R_1 , C_1 , point A, D_1 , point C, to point E. The other one is from the earth ground, passing by R_2 , C_2 , point B, D_3 , point D, point C, to point E. Because both D_1 and D_3 are conducting, the potential of point A is equal to that of point C, while the potential of point B is also equal to that of point D. Therefore, the impedance of two noise paths are almost the same. The noise current can be distributed evenly between the two noise paths.

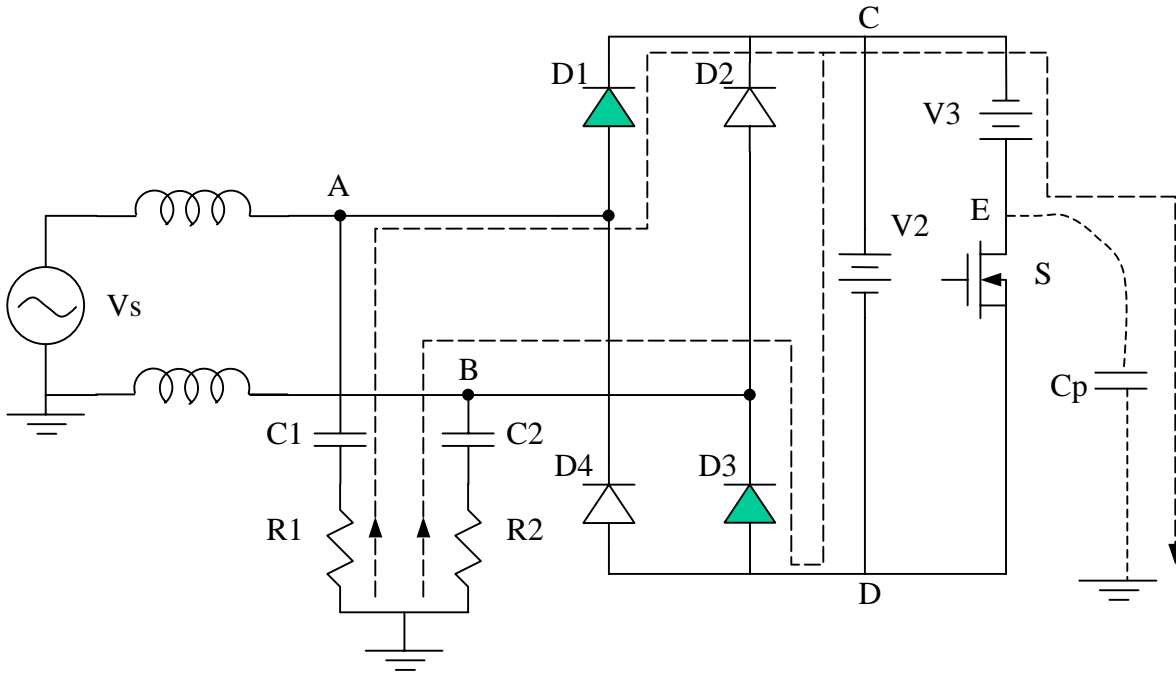


Fig.2-8 Rectifier Diodes On; Switch being Turned Off

Fig.2-9 shows a similar situation when the switch is being turned on and the parasitic capacitance is being discharged. There are also two noise paths. One is from point E, passing by point D, point C, D1, point A, C1, R1, to the earth ground. The other one is from point E, passing by point D, D3, point B, C2, R2, to the earth ground. Because $V_A = V_C$ and $V_B = V_D$, the impedance of two noise paths are almost the same and the noise current can be distributed evenly between the two paths.

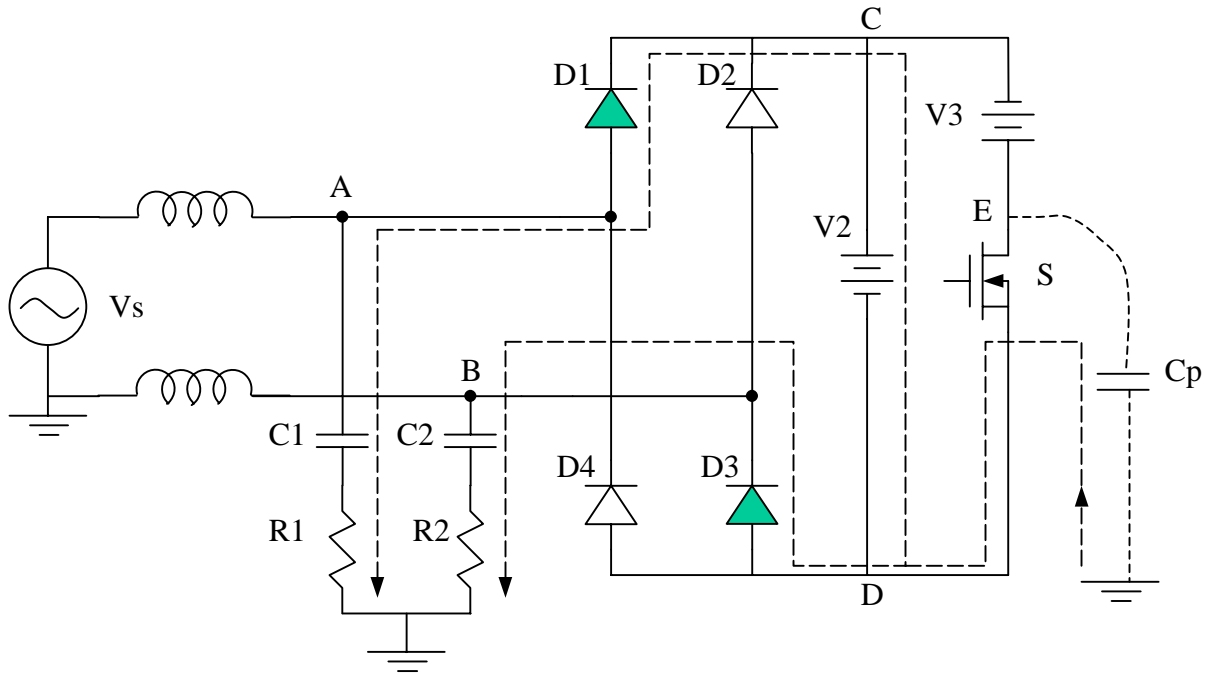


Fig.2-9 Rectifier Diodes On; Switching being Turned On

Regardless of whether the switch is turned on or off, there exist two paths with almost identical impedance as long as two diodes are conducting. So the two currents flowing through the two LISN branches are almost the same. The noise generated in this way is pure CM noise.

2.3.2.2. Rectifier Diodes Off

For the following discussion, we assume $V_2 > V_{AB} > 0$. In Fig.2-10, the switch was originally “on”, $V_E \approx 0V$. When the switch is being turned off, V_3 finds a path to charge the parasitic capacitance C_p . The path is from the earth ground, passing by R1, C1, point

A, D1, point C, to point E. So the potential of point E will be raised from zero to $V_C + V_3$, which is equal to $V_A + V_3$. Since V_C is equal to V_A , V_D is then equal to $V_A - V_2$, which is less than zero. This means D_3 and D_4 are reversed biased. Since only one diode D_1 conducts, there is noise current flowing through only one LISN branch, resulting in differential mode noise, which is NIDM.

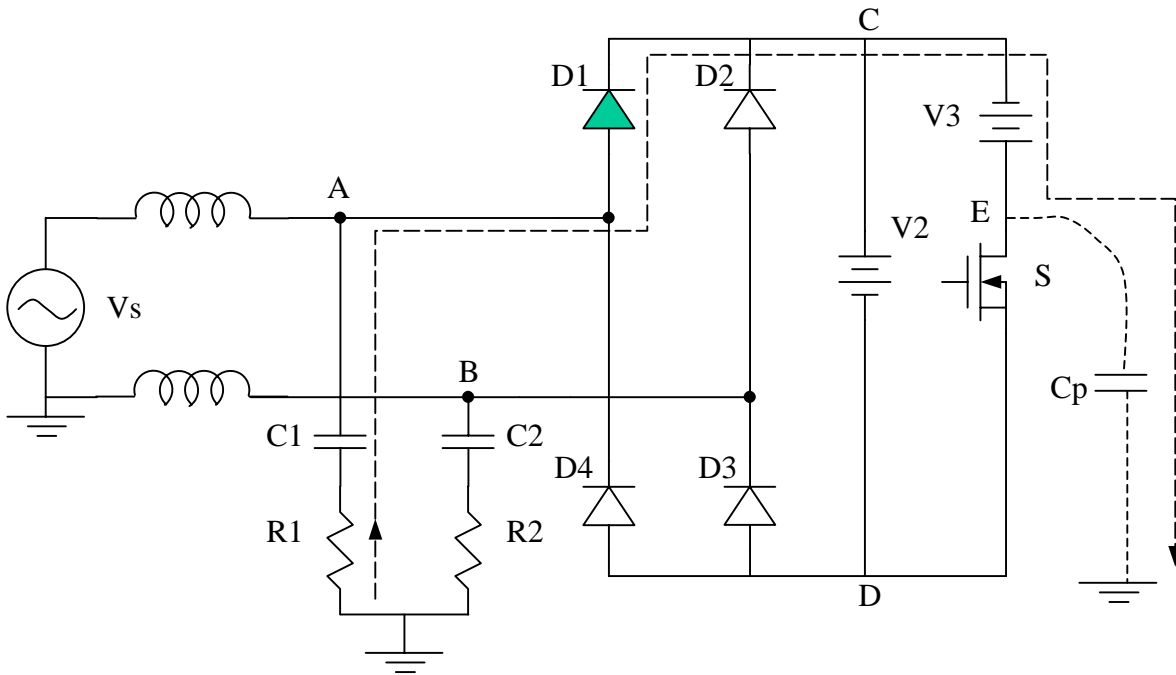


Fig.2-10 Rectifier Diodes Off; Switch being Turned Off

A similar situation is shown in Fig.2-11, the switch was originally in “off” position, $V_E = V_A + V_3 > 0$. When the switch is being turned on, point D is clamped to $V_A + V_3$ instantaneously, resulting the discharge of parasitic capacitance C_p . The discharge path is from point E, passing by point D, D_3 , point B, C_2 , R_2 , to the earth ground. Now the potential of point D is zero, so V_C is equal to V_2 . Diodes D_1 and D_2 are being reverse biased. Again there is only one diode D_3 conducting. The noise current will only flow

through one branch of LISN. Because of unbalanced current flow through the two branches of the LISN, DM noise can be measured.

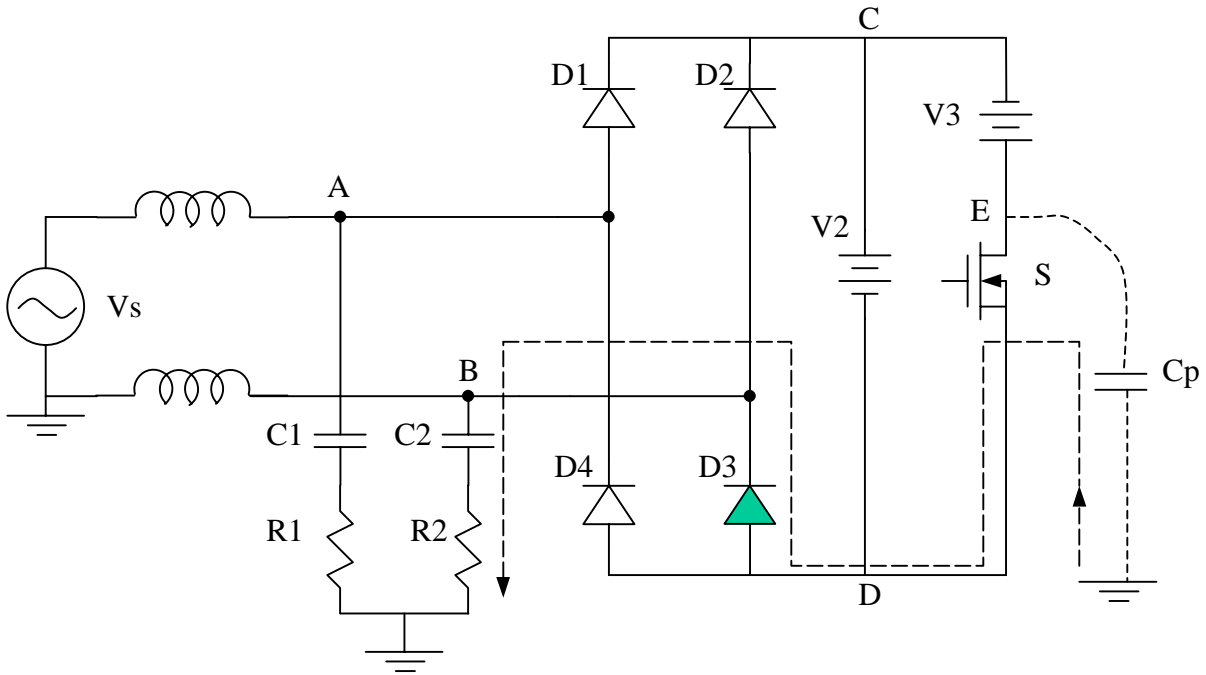


Fig.2-11 Rectifier Diodes Off; Switch being Turned On

This kind of DM noise is different from conventional DM noise because it is not related to the input current harmonics. It is related to the charging and discharging of the parasitic capacitance.

2.4 Basic Characteristics of NIDM

The relationship of NIDM noise with input line voltage and load current will be discussed in this section.

2.4.1 Dependency of NIDM on Line Voltage

Similar to CM noise, NIDM noise is a voltage-generated phenomenon. The noise current is mainly determined by dv/dt across the parasitic capacitance. Higher input line voltage will lead to higher dv/dt . Therefore, the amplitude of NIDM emission is dependent on the input line voltage, i.e. the higher the input line voltage, the larger the NIDM emission. The above conclusion can be verified by experiments. Fig.2-12 shows the NIDM noises observed in zero-span mode. The central frequencies and load conditions are the same for both cases. The only difference is the input line voltage. A 100 W offline flyback switching power supply was used in the measurement. The output voltage is 5 V DC and the output power is 50 W for both cases. The central frequency is also the same (230kHz) for both cases. But the input line voltage is 120 V AC for the first case and is 70 V AC for the second case.

We can see clearly that the input voltage has much more effect on NIDM than on IDM. Basically IDM is affected by input voltage with minor effect.

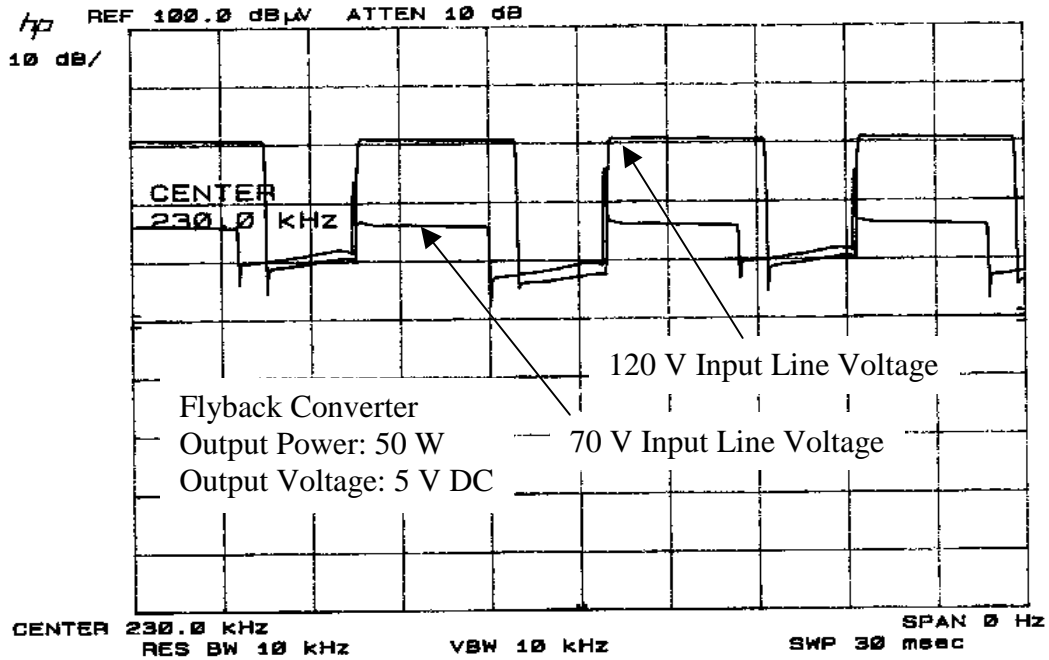


Fig.2-12 NIDM at Different Line Voltages

2.4.2 Dependency of NIDM on Load Current

NIDM is a voltage-generated phenomenon as opposed to a current-generated phenomenon in IDM noise, so the input line voltage, not the input current, determines the absolute amplitude of NIDM. Load current (or the input current) can affect NIDM noise with minor effect. As shown in Fig.2-13, under heavy load condition, the rectifier diode conduction period is longer than the diode off period. The time interval occupied by IDM (period a) is longer than that occupied by NIDM (period b). But under light load condition, the diode conduction period is shorter than the diode off period. In one line cycle, the interval occupied by NIDM is longer than the other interval occupied by IDM. As can be seen from the oscillogram, load changes the IDM much more than NIDM

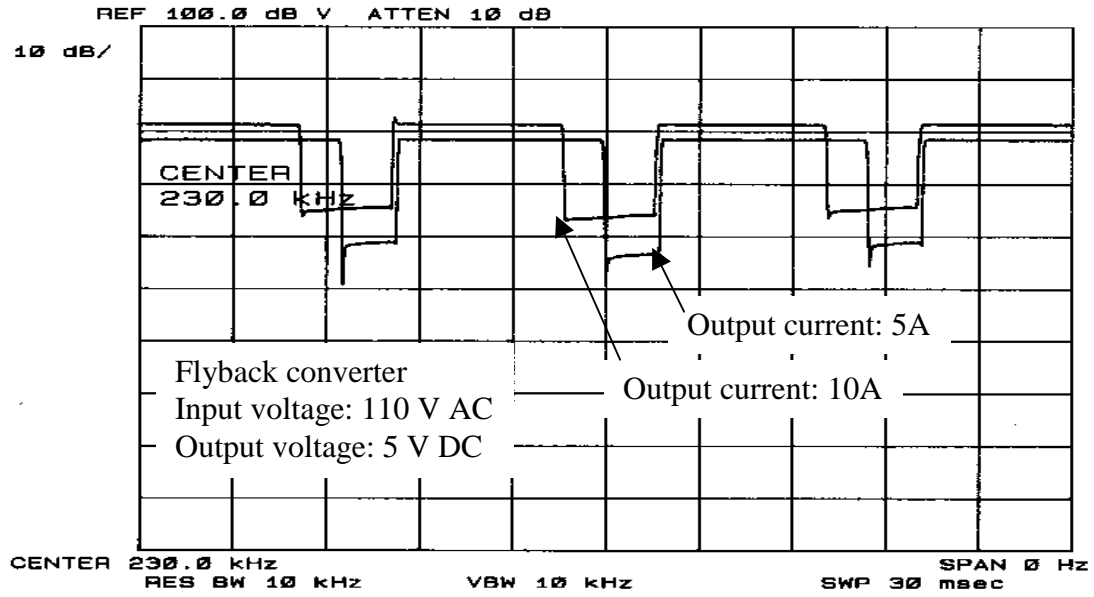


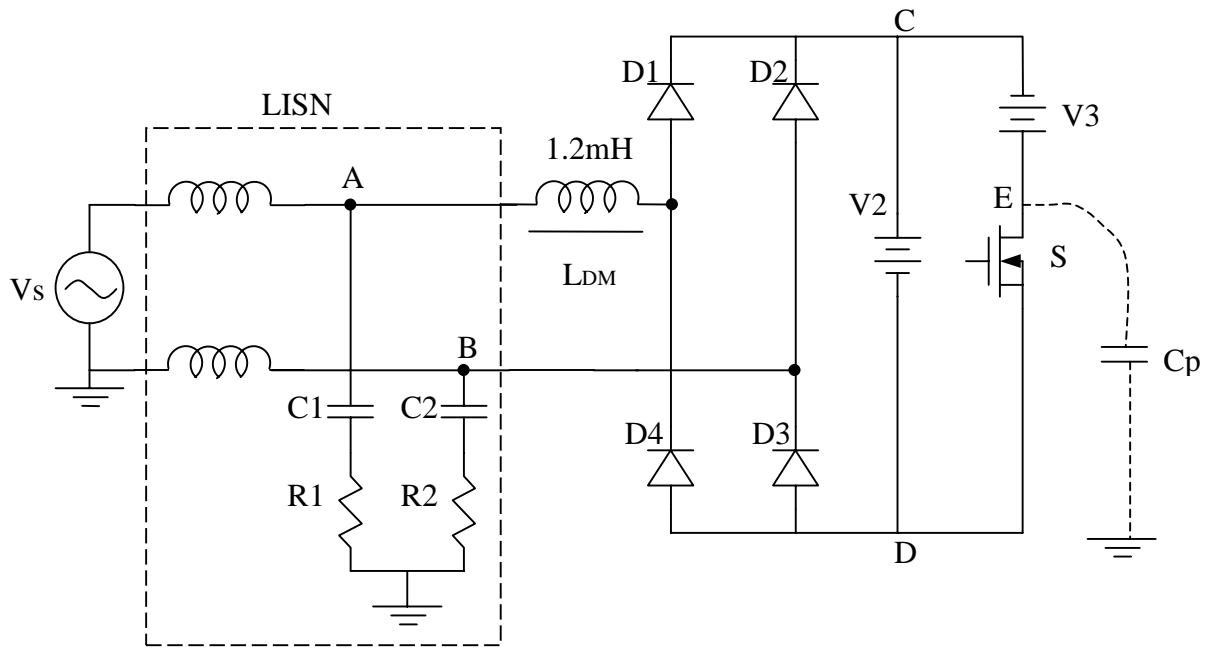
Fig.2-13 NIDM at Different Load Currents

Chapter 3 Implications of NIDM to EMI Filter Design

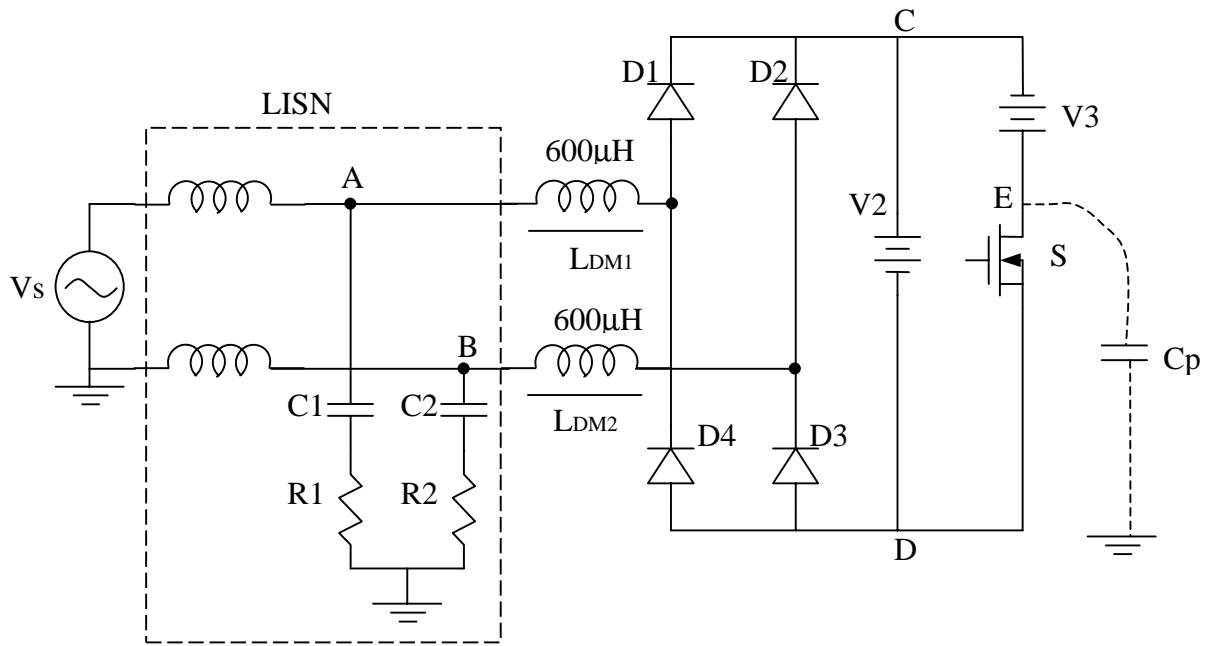
In this chapter, the implications of non-intrinsic differential mode (NIDM) noise to EMI filter design will be discussed. Many puzzles commonly encountered in EMI filter design can be explained with NIDM phenomenon. Means to attenuate NIDM are also described in this chapter. An understanding of NIDM has practical implications on filter design.

3.1 Asymmetrical DM Choke vs. Symmetrical DM Choke

NIDM noise can be generated during the bridge rectifier “off” period. As we discussed before, there are two paths for the ground noise current. When the rectifier is off, the line impedance of one noise path is much higher than the other one. Therefore, the asymmetry of noise path impedance causes most of the noise current flowing through the low impedance path and DM noise is generated. Actually, the unbalance of the noise path can also be attributed to asymmetry of filter topology. One example is the DM choke in a filter. Fig.3-1 shows the power circuit and the two possible filter topologies.



(a) Asymmetrical DM Choke



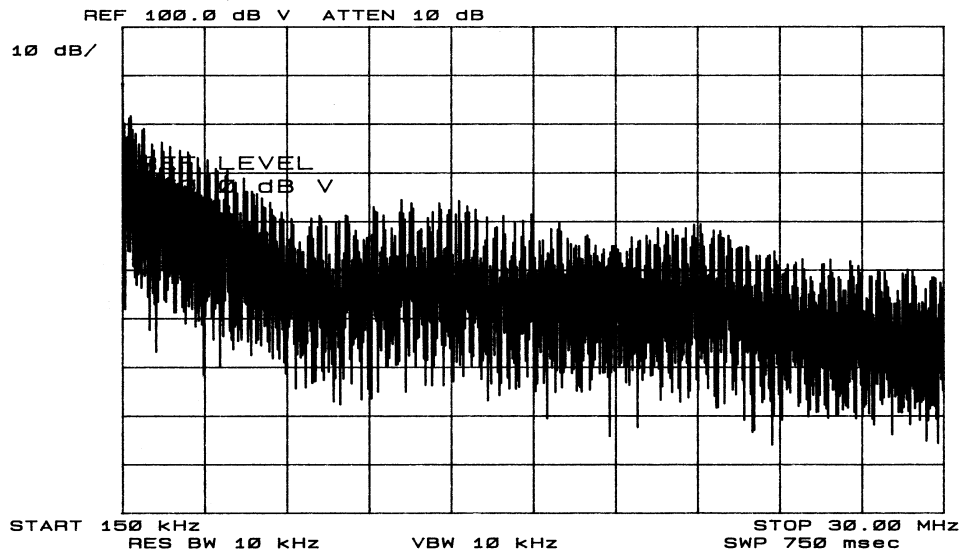
(b) Symmetrical DM Choke

Fig.3-1 Test Setup of Asymmetrical Filter

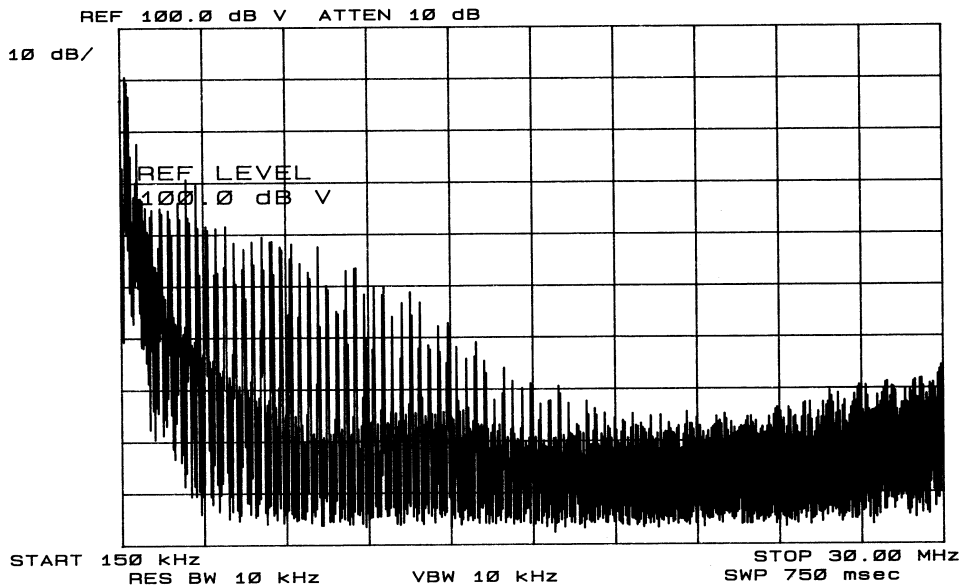
The only difference between Fig.3-1 (a) and (b) is that asymmetrical DM choke is used in Fig.3-1 (a) and symmetrical one used in (b). Notice that the total inductance of the two chokes in Fig.3-1 (b) is the same as that of the single choke in Fig.3-1 (a). No other filter elements are used.

3.1.1 Description of Phenomenon

According to conventional conducted EMI emission theory; the DM noise attenuation of the two filter topologies should be the same because of the same inductance values. However, the experimental result of Fig.3-2 shows otherwise. Fig.3-2 (a) is the total DM noise spectrum of the EUT with one 1.2mH DM choke on one side. Fig.3-2 (b) is the DM noise of the same EUT with two 600 μ H DM chokes on both sides. It shows clearly that the noise amplitude in the symmetrical choke case is lower than that of the asymmetrical case. This phenomenon cannot be explained by the conventional conducted EMI theory. In the next section, NIDM noise theory discussed in Chapter 2 will be used to analyze that phenomenon.



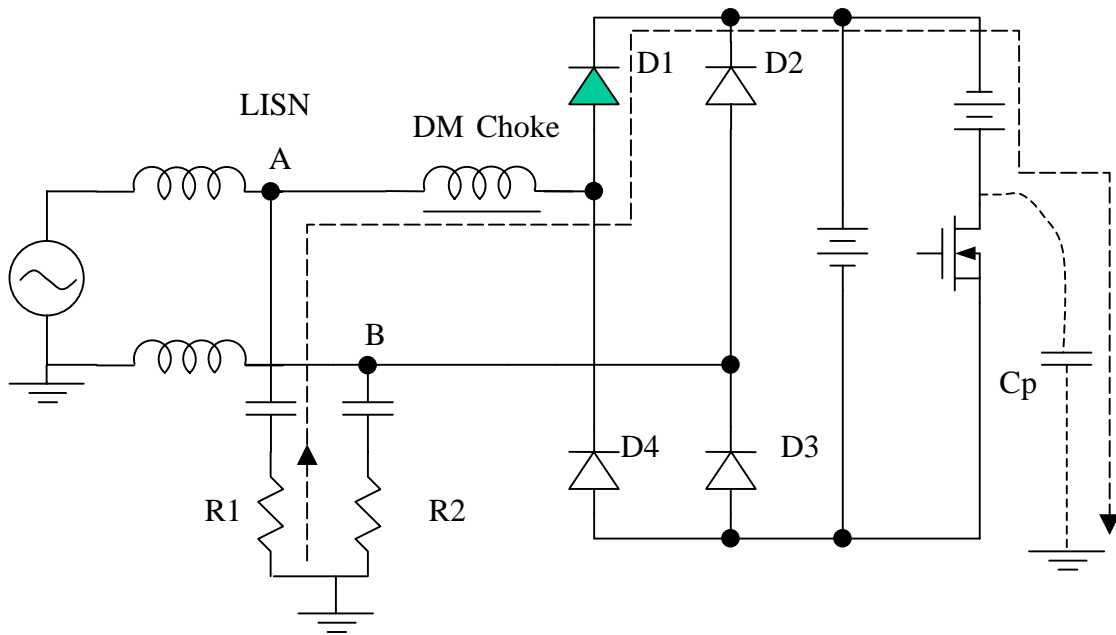
(a) DM Noise with Asymmetrical DM Choke



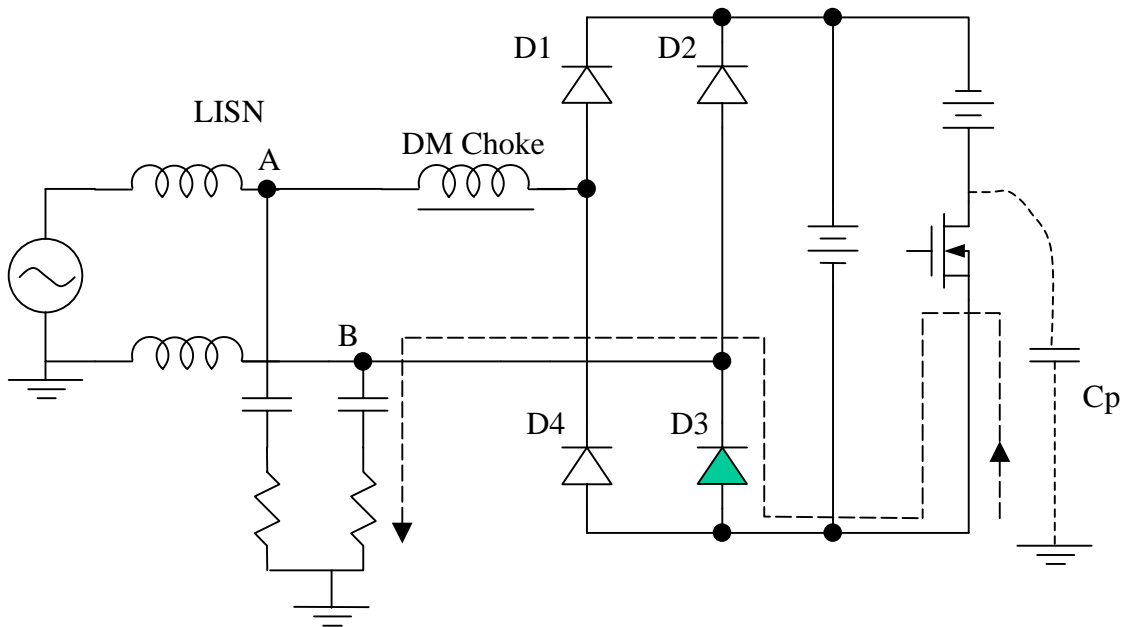
(b) DM Noise with Symmetrical DM Choke

Fig.3-2 Asymmetrical DM Choke vs. Symmetrical DM Choke

3.1.2 Effect of Asymmetrical DM Choke



(a) Rectifier Diodes Off, MOSFET Being Turned On (C_p Discharged)



(b) Rectifier Diodes Off, MOSFET Being Turned Off (C_p Charged)

Fig.3-3 Noise Path Models with Asymmetrical DM Chokes

The phenomenon can be explained from the noise model shown in Fig.3-3. Fig.3-3 (a) shows the case of asymmetrical DM choke when MOSFET is being turned off and parasitic capacitance C_p is being charged. The charging current flowing through R1 sees the inductance and the noise current can be suppressed. Fig.3-3 (b) shows the situation when rectifier is “off” and MOSFET is being turned on. Noise paths are unbalanced and NIDM still exists. Notice that most of the ground noise flows through D3 and R2 without seeing DM inductor. Therefore, the DM choke has no attenuation for the noise in that case. Fig.3-4 shows that although IDM can be suppressed by the asymmetrical DM choke, the amplitude of NIDM does not change. If NIDM is dominant in total DM spectrum, then the DM noise envelope will not change after the use of an asymmetrical DM choke.

Notice that the two waveforms are supposed to coincide on both trailing edges. In fact, the waveform marked as “DM with asymmetrical choke” was purposely displayed with some delay to see the waveforms better.

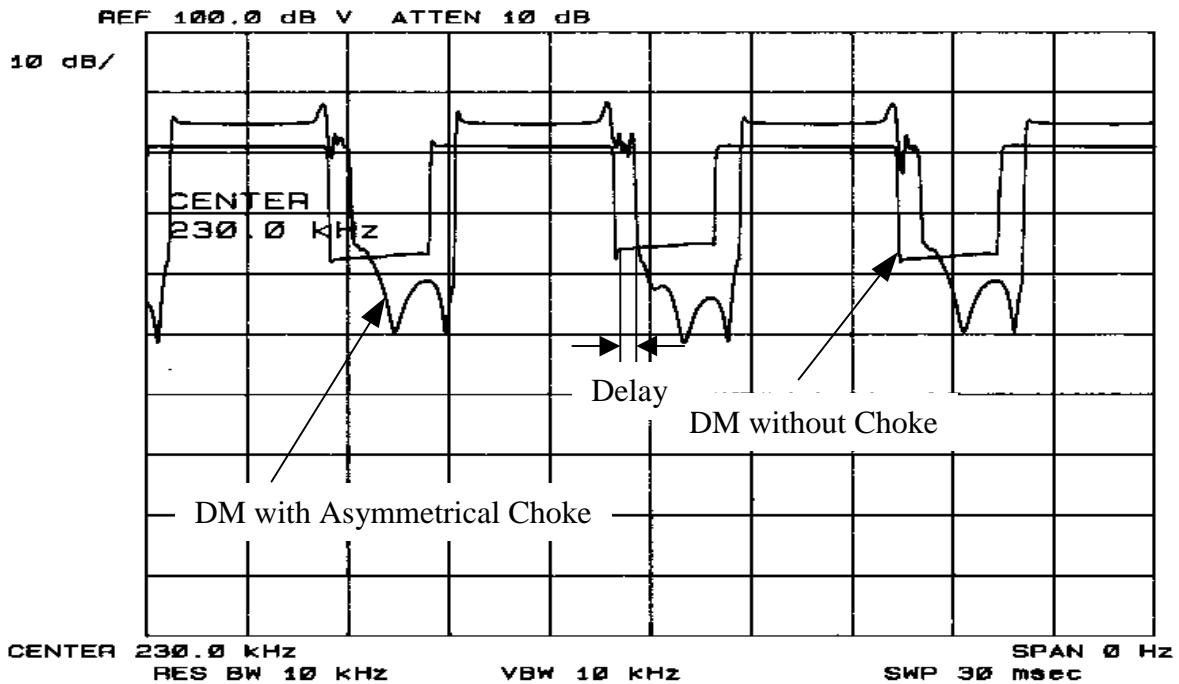
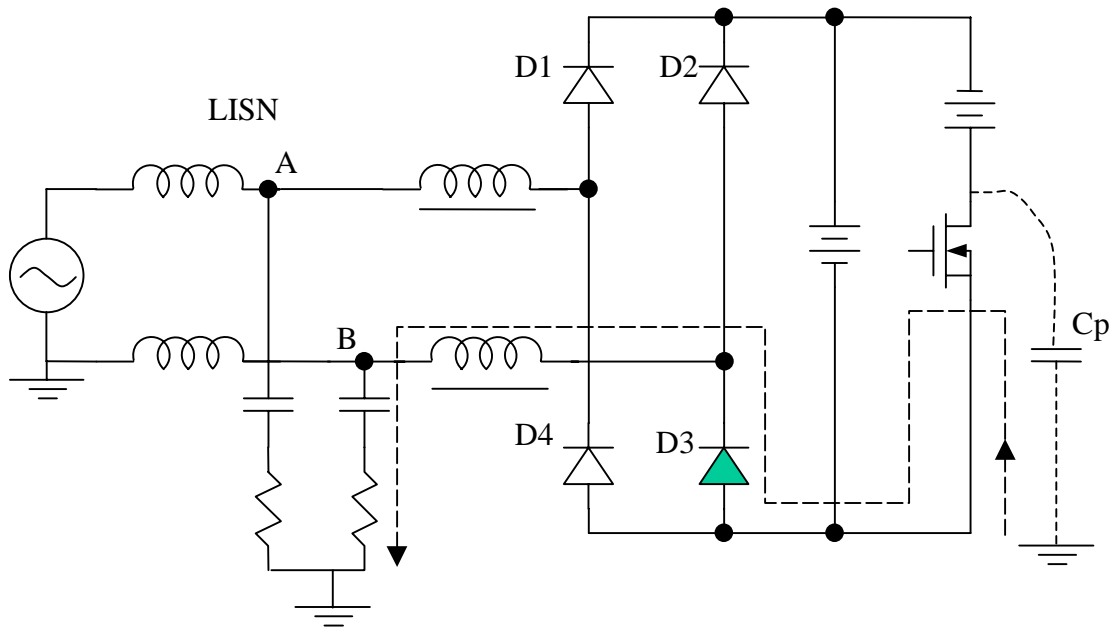


Fig.3-4 DM Noise with Asymmetrical DM Choke (Zero Span Mode)

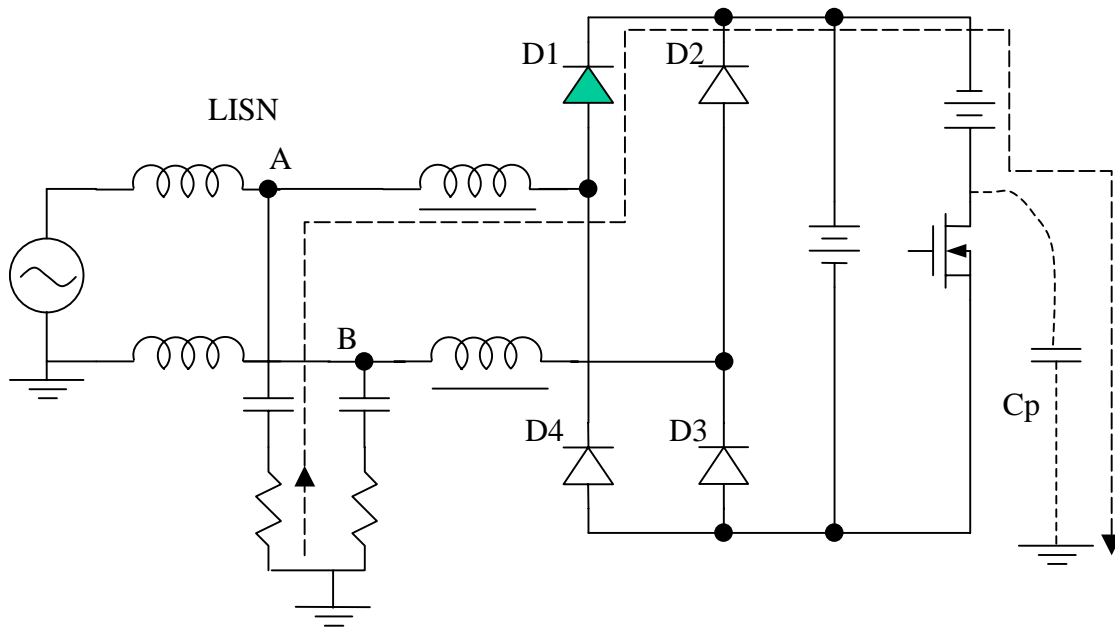
The waveform of “DM with asymmetrical choke” was purposely delayed for the convenience of observation.

3.1.3 Effect of Symmetrical DM Choke

From above analysis, we know that asymmetrical filter topology can also contribute to the generation of NIDM. To verify this conclusion, we split the 1.2mH DM choke into two 600 μ H chokes as shown in Fig.3-1 (b). From Fig.3-2 (b), we can see DM noise attenuation of the symmetrical filter topology is significant, especially for high frequency range. This can also be explained using noise path models shown in Fig.3-5. Fig.3-5 (a) shows the situation when rectifier diodes are off and the MOSFET is being turned off.



(a) Rectifier Diodes Off, MOSFET Being Turned Off (C_p Discharged)



(b) Rectifier Diodes Off, MOSFET Being Turned Off (C_p Charged)

Fig.3-5 Noise Path Models with Symmetrical DM Chokes

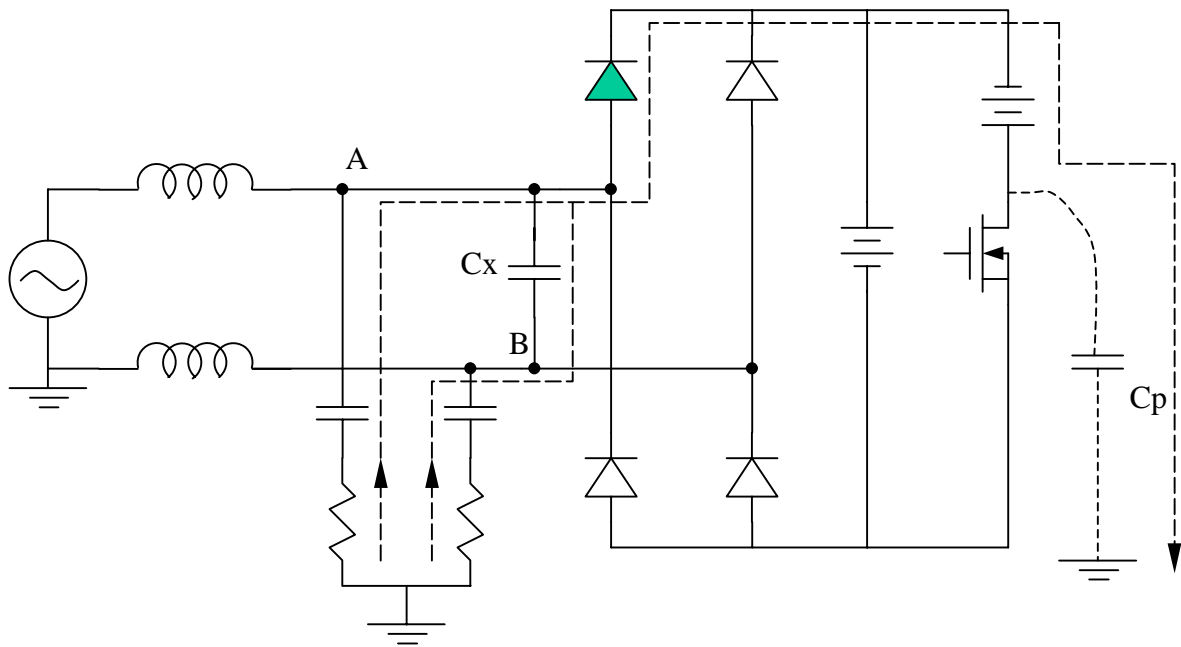
Fig.3-5 (b) illustrates the situation when rectifier diodes are off and the MOSFET is being turned off. The noise paths are unbalanced in this case. But we can see no matter which path the noise current takes, it will always see a DM choke in the path and the ground noise current can then be suppressed by the inductance.

This conclusion is extremely critical to filter design. When designers choose filter topologies, they usually do not pay much attention to the symmetry of the filter, even though they know empirically that symmetrical topology is better than asymmetrical one. The above experiment has demonstrated clearly the advantage of symmetrical filter topology in suppressing NIDM.

3.2 Effect of X Capacitor on NIDM

The NIDM noise discussed so far is of the same generation mechanism: the impedance unbalance of the two noise current paths during rectifier diodes “off” period. If the impedance of one path is much higher than that of the other path, more noise current will flow through the lower impedance path and cause higher voltage drop across one of the LISN resistors. DM noise is defined earlier as the difference between the noise voltages across both LISN branches ($DM = (V_x - V_y)$). Therefore, a significant amount of DM noise will be measured if the noise paths are unbalanced. The best way to filter this noise is to balance the noise current paths so that the current can be distributed evenly between both LISN resistors during parasitic capacitor C_p charging and discharging.

To balance the two current paths, a capacitor C_x , which is usually known as X capacitor can be connected between points A and B as shown in Fig.3-6 (a) and Fig.3-6 (b). For high frequency noise current, the impedance of the capacitor is very low. C_x is essentially shorted if the capacitance is large enough. The unbalanced situation described above can be corrected because high frequency noise current can flow evenly through both of the LISN branches during both MOSFET “on” and “off” transients. The paths for ground noise current will become balanced. The noise voltage difference between the two LISN branches is small and the NIDM noise is attenuated significantly.



(a) Rectifier Diodes Off, MOSFET Being Turned Off (C_p Charged)

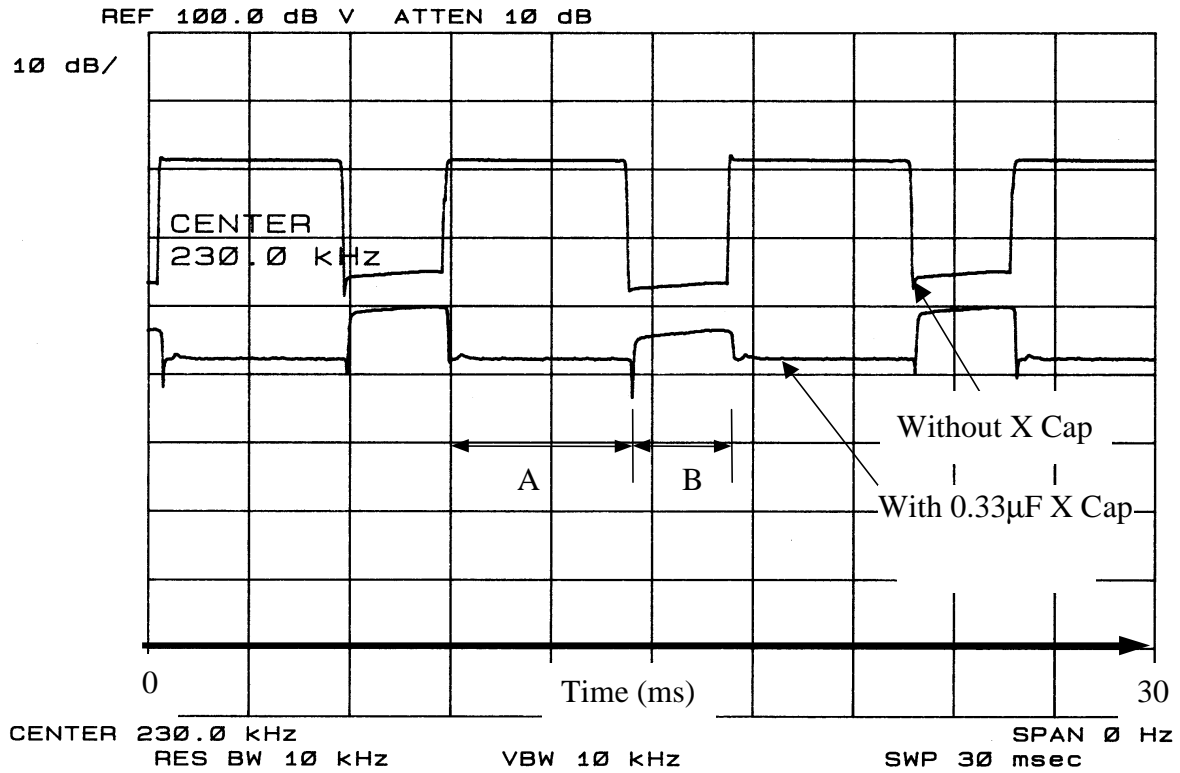
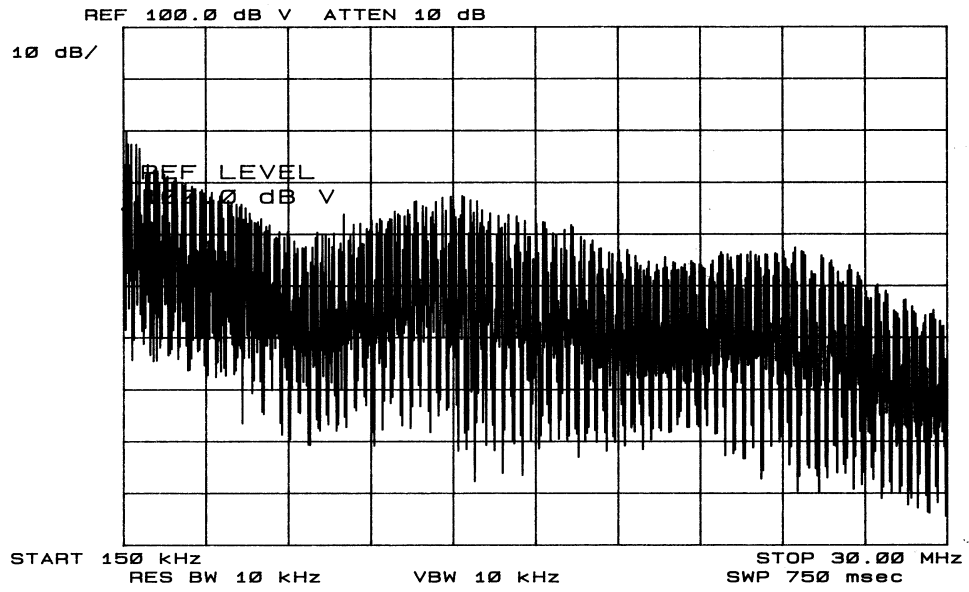


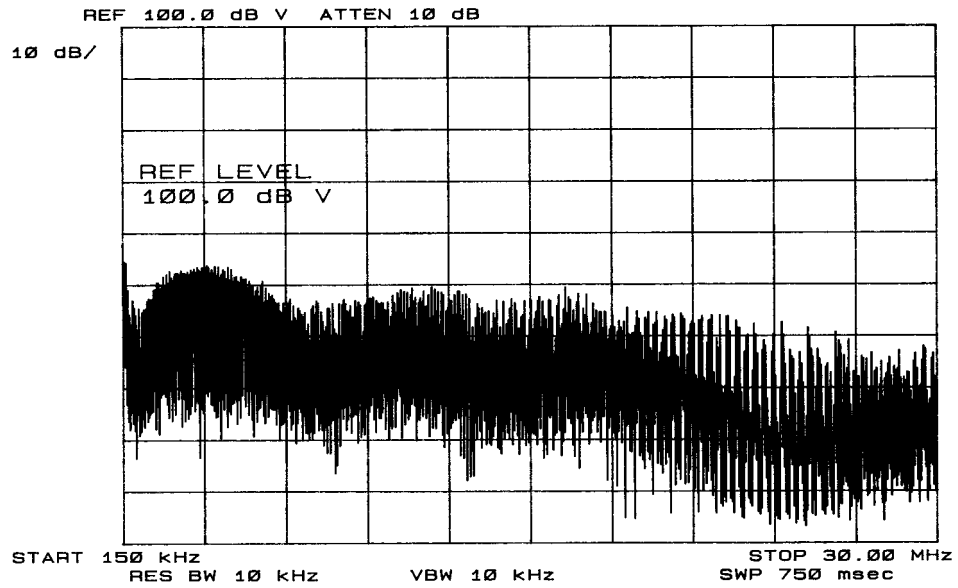
Fig.3-7 Effect of X Capacitor on NIDM in Zero Span Mode

Interval A: Rectifier Diodes Off (NIDM)

Interval B: Rectifier Diodes On (IDM)



(a) DM Noise without X Capacitor

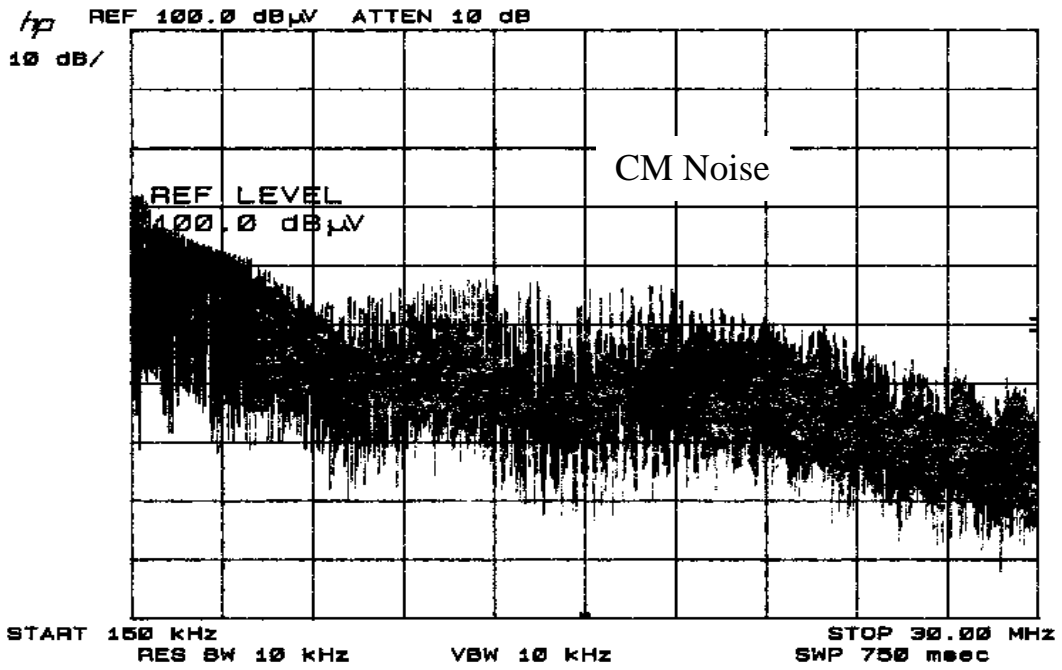


(b) DM Noises with X Capacitor

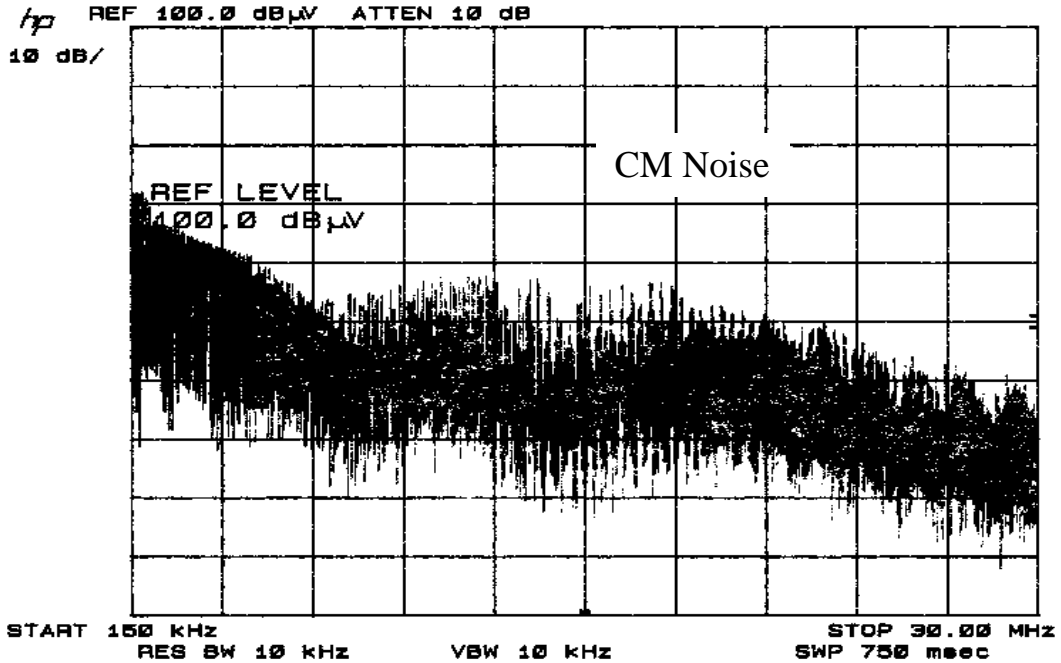
Fig.3-8 Effect of X Capacitor on NIDM in Frequency Domain

From Fig.3-7, We can see the X capacitor has little attenuation on IDM (less than 3 dB). This can be justified by the characteristics of IDM noise source. The noise source impedance of IDM is usually very low, so a capacitor in parallel is not effective as an inductive filter. However, the attenuation for NIDM is significant (almost 15 dB) because of the balanced noise paths. The total DM reduction after adding C_x is shown in Fig.3-8. The DM noise reduction after adding X capacitor is very significant. To balance the noise current paths, the impedance of the X capacitor should be as low as possible. But on the other hand, lower impedance means higher capacitance value and larger size, which is undesirable in filter design. That issue will be addressed in Section 3.5 of this chapter.

Another question regarding balancing noise paths with X cap is: “Does adding X cap increase the CM noise?” Because it seems like the X cap changes NIDM into CM. The answer to that question is no. Fig.3-9 shows the CM measurement results before and after adding X cap. CM noise level keeps to be the same for both cases. CM noise is the average of V_x and V_y . In unbalanced case, one voltage is much higher than the other one. When the noise paths are balanced, the two voltages become the same value. But the summation of these two voltages will not change because during steady state operation, the total charge of the parasitic capacitor C_p is constant for each switching cycle.



(a) CM Noise without X Capacitor



(b) CM Noise with X Capacitor

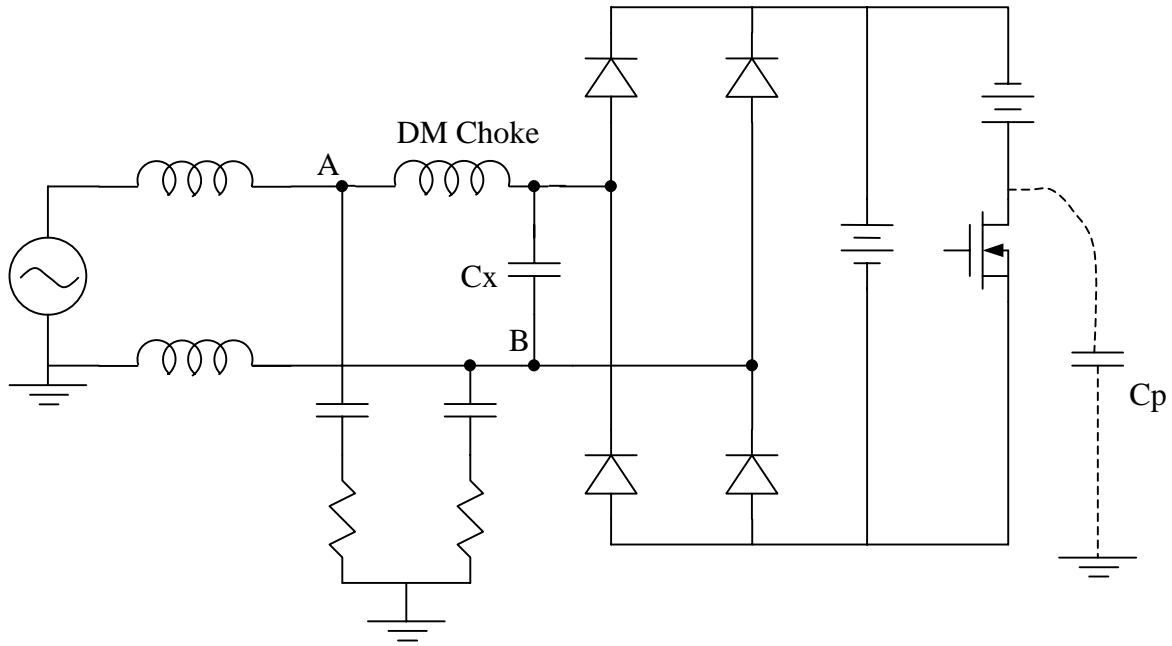
Fig.3-9 Effect of X Capacitor on CM Noise

3.3 Position of X Capacitor in Filter

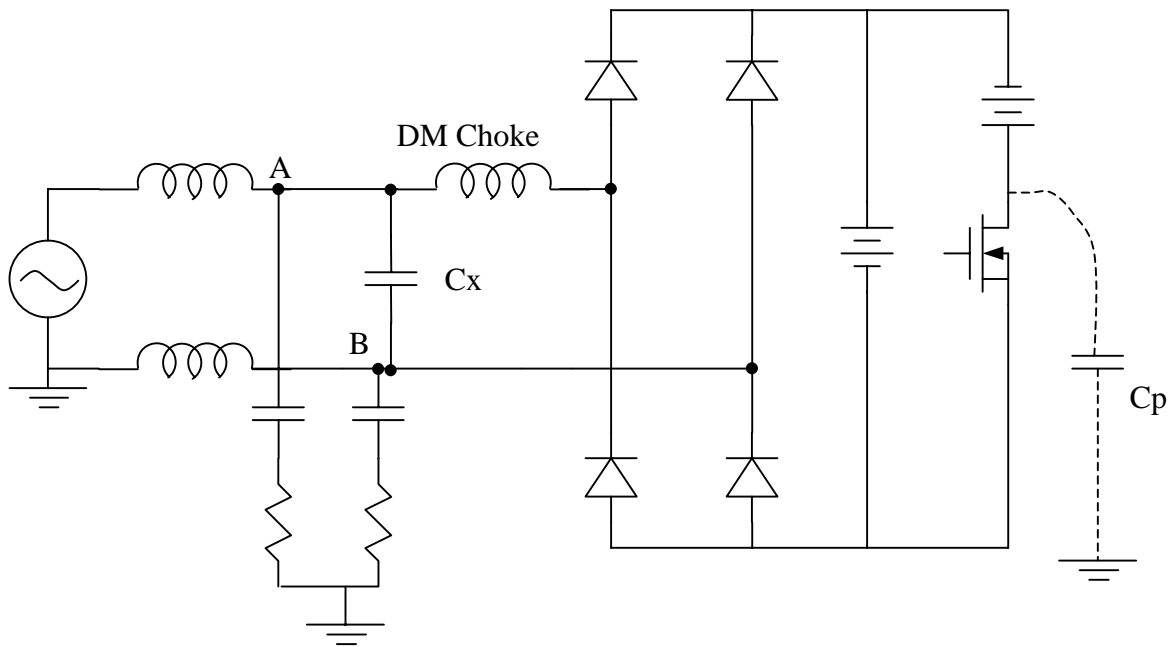
The use of X capacitors can effectively attenuate NIDM noises caused by noise path unbalance as discussed in Section 3.2. But from earlier discussion, we know X capacitor by itself has little attenuation effect on IDM noise that is usually caused by the harmonic-rich input current. Other filter elements must be used together with the X capacitor to get a better suppression of all the DM noise components. Because of the low source impedance nature of IDM noise, the filter for IDM must consist of at least one inductive element. A commonly asked question is: if such an inductor-capacitor filter topology is used, should the X capacitor be placed on the LISN side or on the EUT side of the circuit? The answer is that it depends on whether symmetrical choke or asymmetrical choke is used. This will be discussed below

3.3.1 Asymmetrical Inductor with X Capacitor

The DM filter consists of two components: a single-side DM asymmetrical choke and an X capacitor. There are two possible filter topologies depending on the position of X capacitor. In one topology, the X capacitor is adjacent to EUT and in the other, X capacitor is right next to LISN as shown in Fig.3-10(a) and Fig.3-10(b). To distinguish these two topologies, we call the first one “LC” filter and the second one “CL” filter.



(a) X Capacitor on EUT Side (LC Filter)

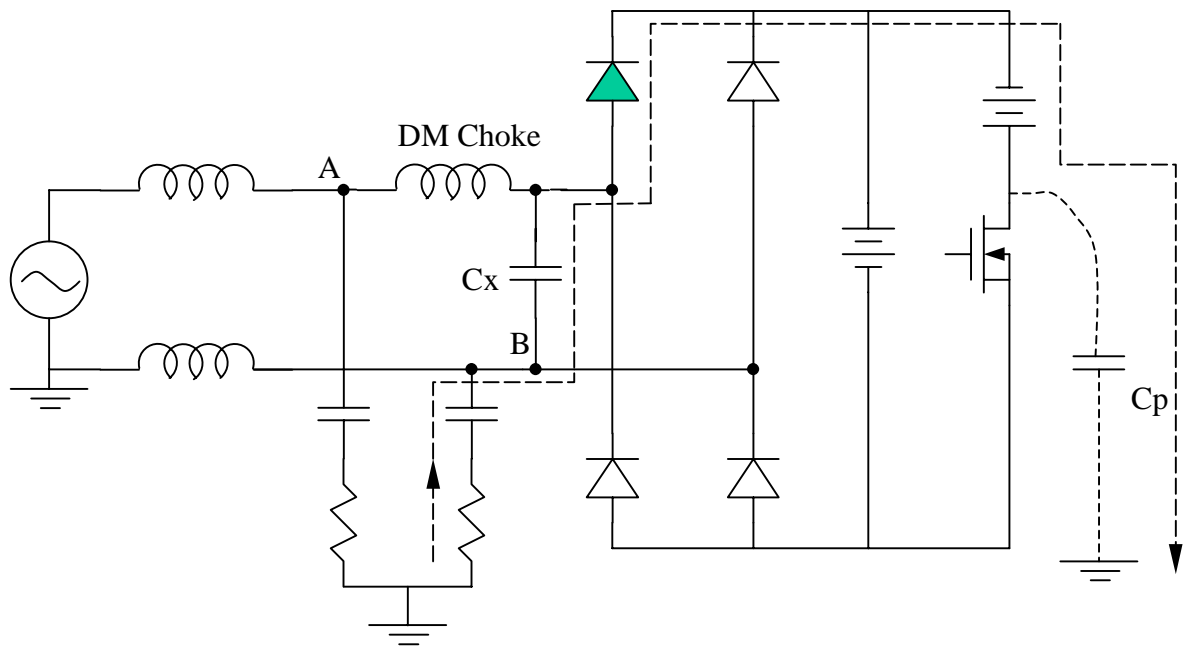


(b) X Capacitor on LISN Side (CL Filter)

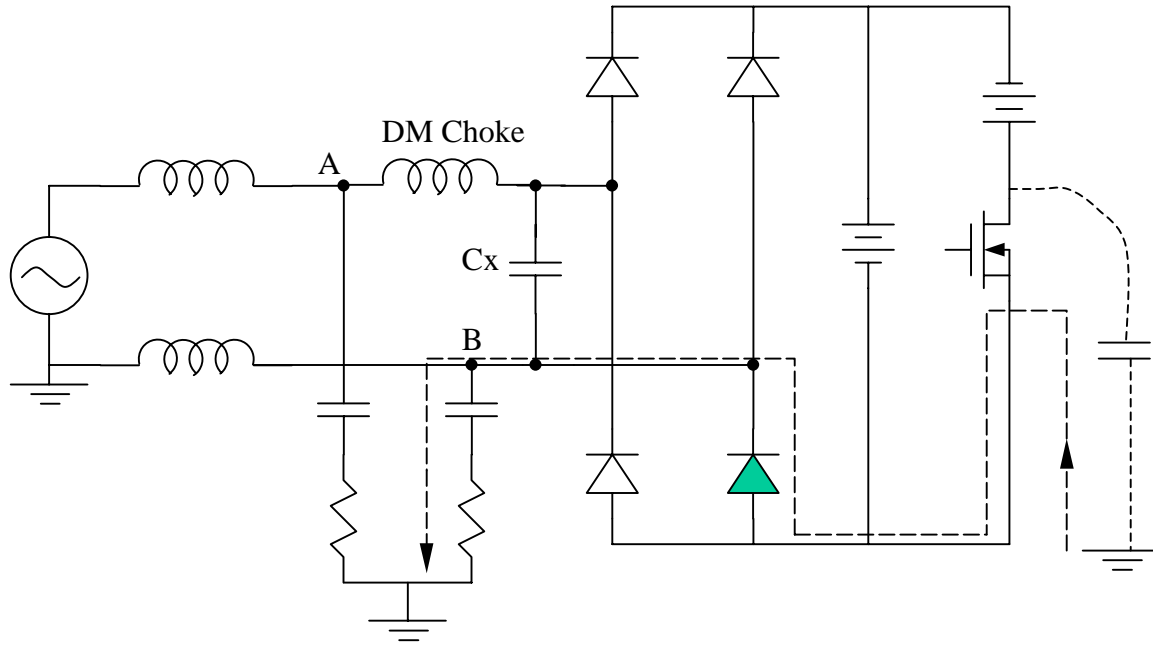
Fig.3-10 Two Asymmetrical DM Filter Topologies

3.3.1.1 Asymmetrical Filter Topology with X Cap on EUT Side

First, consider the topology with X capacitor adjacent to EUT. Using a simplified noise emission model shown in Fig.3-11 (a) and Fig.3-11 (b), the ground noise current paths can be found.



(a) Switch Being Turned Off (C_p Charged)



(b) Switch Being Turned On (C_p Discharged)

Fig.3-11 Noise Path Model: Asymmetrical DM Choke, X Capacitor on EUT Side,
Rectifier Diodes Off in Both Cases

Fig.3-11 (a) shows the NIDM noise path when the switch is being turned off and (b) shows the noise path when the switch is being turned on. It can be seen that no matter whether the switch is being turned on or off, the two noise current paths have different impedance values even though the X capacitor has been added. The difference in impedance values is caused by the existence of asymmetrical DM choke. The noise path with DM choke is higher in impedance and less noise current and the other path is lower in impedance and more noise current flowing through. The noise current difference between these two paths becomes NIDM noise. Fig.3-12 is the DM noise captured with zero-span mode. The upper trace was measured when only a DM choke was inserted

between LISN and EUT. The lower trace was measured when both DM choke and an X capacitor were used, and the X capacitor is next to EUT. Again, the shift of the bottom waveform is purposely done for better view of the two waveforms. One can see from this figure that NIDM part is reduced by some amount but not much.

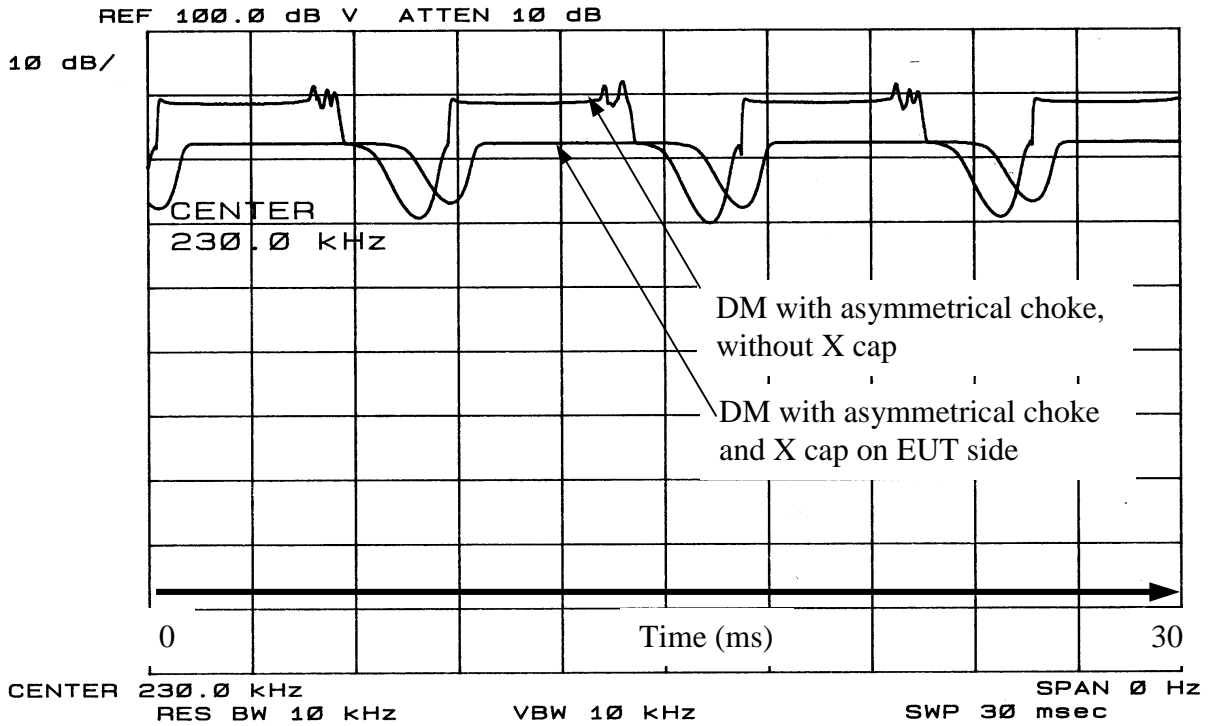
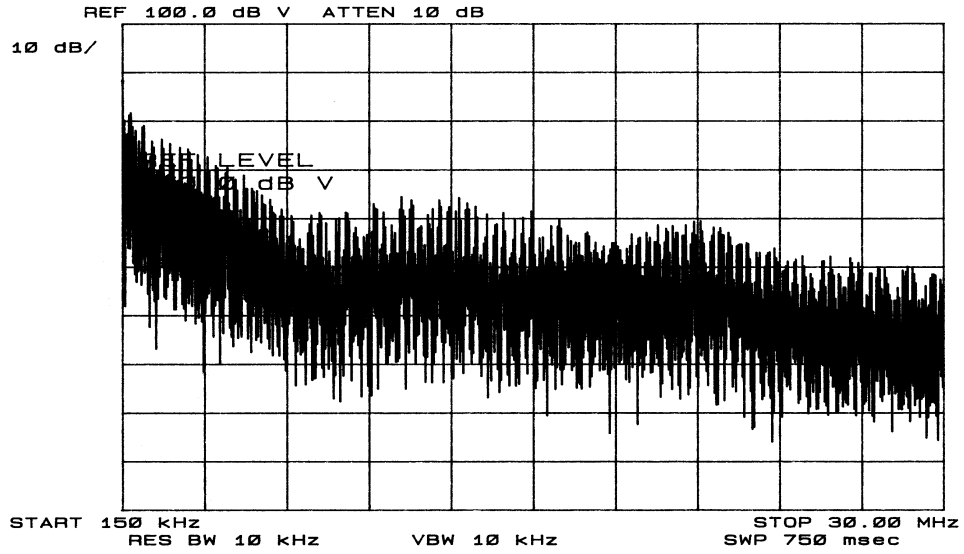
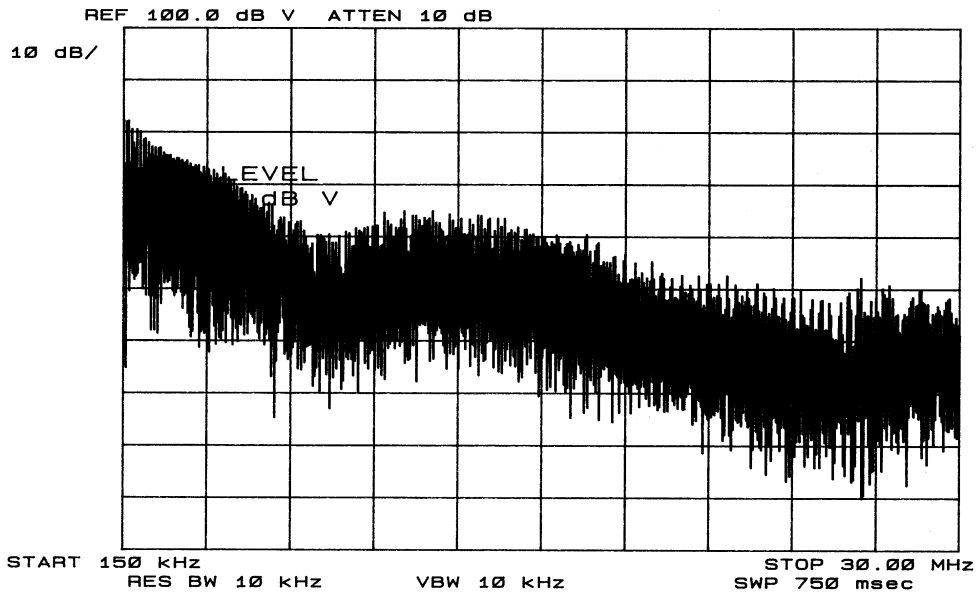


Fig.3-12 DM with Asymmetrical Choke and X Cap on EUT Side

From Fig.3-12, we can see the reduction of NIDM noise is not obvious after adding an X capacitor. The total frequency domain spectrum of DM noise also gives us the same result, which is shown in Fig.3-13.



(a) DM Noise with Asymmetrical DM Choke (No X Cap)



(b) DM Noise with Asymmetrical DM Choke and X Capacitor on EUT Side

Fig.3-13 DM Noise with Asymmetrical Choke and 0.33 μ F X Cap on EUT Side

3.3.1.2 Asymmetrical Filter Topology with X Cap on LISN Side

Consider the topology with X capacitor on LISN side. The noise paths are shown in Fig.3-14(a) and Fig.3-14 (b).

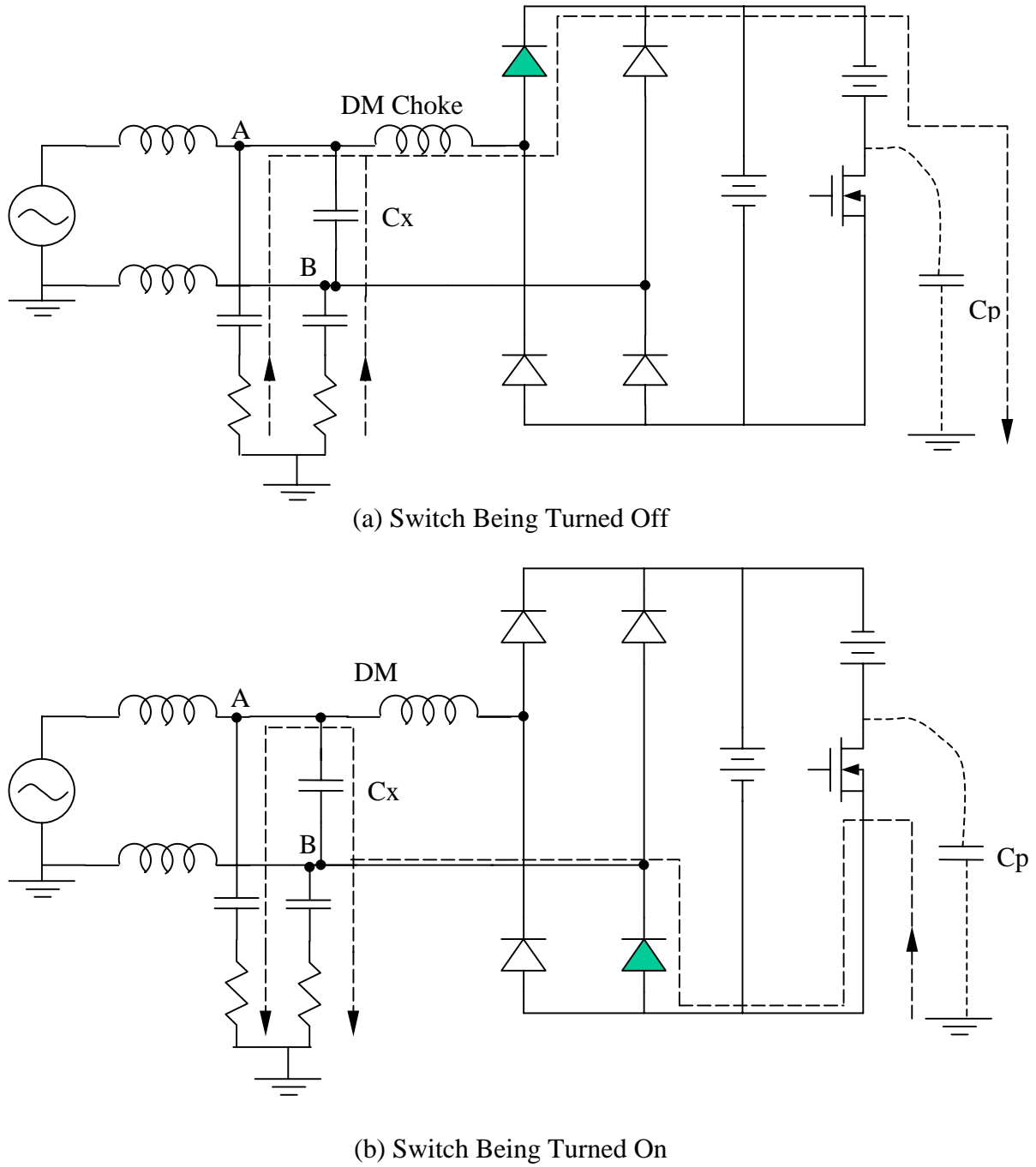


Fig.3-14 Noise Path Model: Symmetrical Choke and X Cap on LISN Side

Fig.3-14 (a) shows the noise path when the switch is being turned off and (b) shows the noise path when the switch is being turned on. It can be seen that whether the switch is being turned on or off, the noise current paths have almost the same impedance values. Adding an X capacitor right next to the LISN reduces NIDM noise much more effectively than otherwise. Fig.3-15 is the DM noise captured with zero-span mode of spectrum analyzer. The upper trace was measured when only a DM choke was inserted between LISN and EUT. The lower trace was measured when both DM choke and X capacitor were used, and the X capacitor is next to LISN. The NIDM reduction is significant (about 30dB compared to 6dB in Fig.3-12).

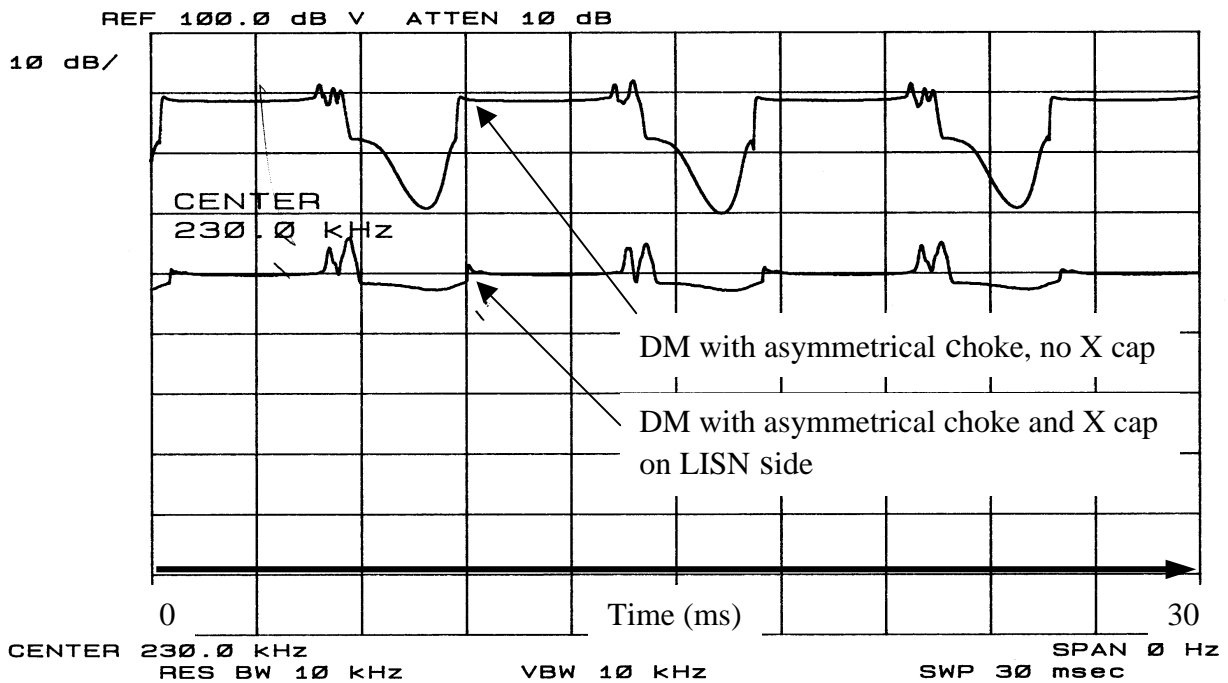
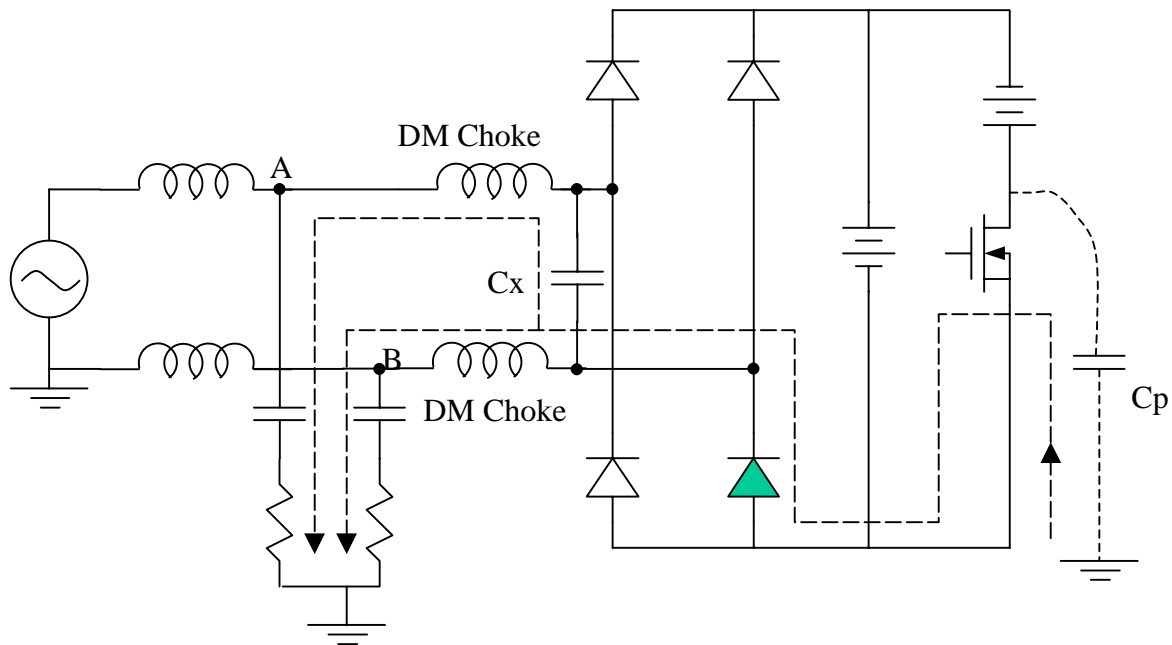


Fig.3-15 DM with Asymmetrical Choke and X Cap at LISN Side (Zero-Span Mode)

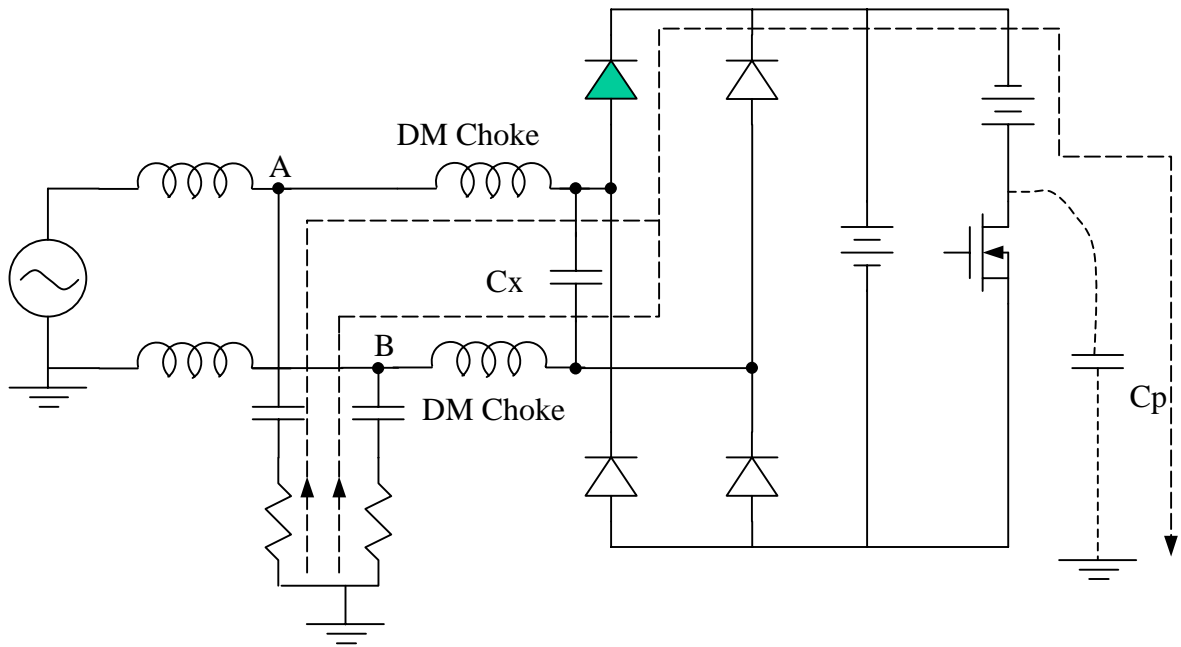
As a conclusion, it is shown that placing the X capacitor on the LISN side is more effective to suppress the NIDM than otherwise if asymmetrical choke is used.

3.3.2 Symmetrical Inductor with X Capacitor

Fig.3-16 and Fig.3-17 show the noise current paths for the two possible filter topologies with a symmetrical DM choke are used. The X capacitor is put on EUT side in Fig.3-16 and on LISN side in Fig.3-17.

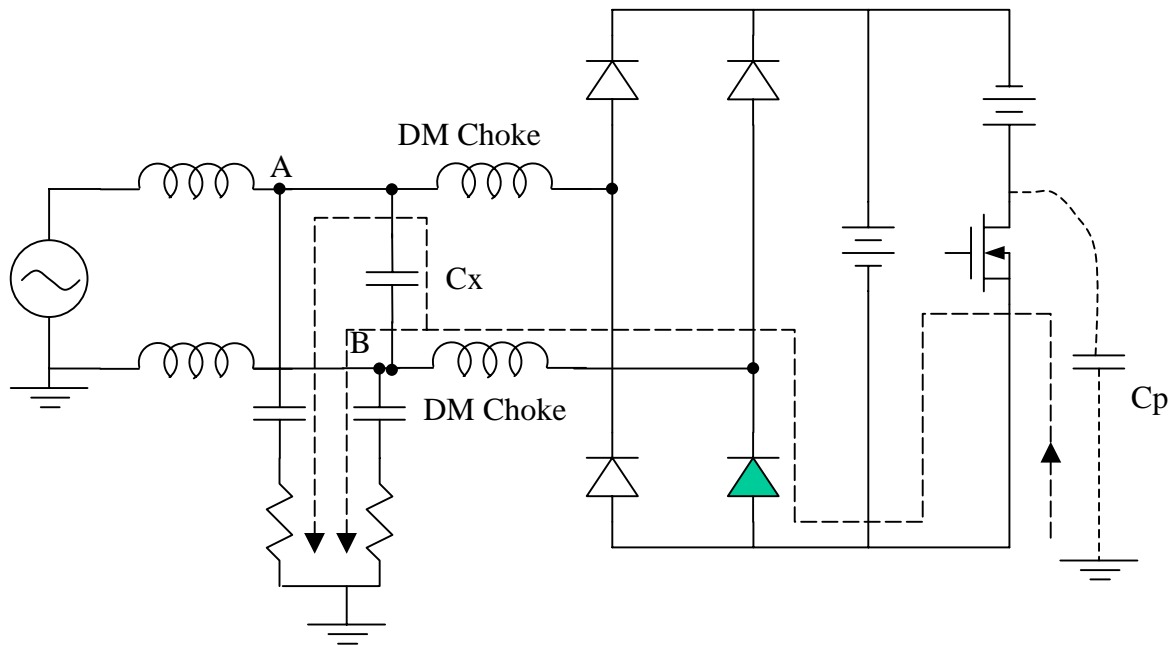


(a) Rectifier Diodes Off, MOSFET Turned On (C_p Discharged)

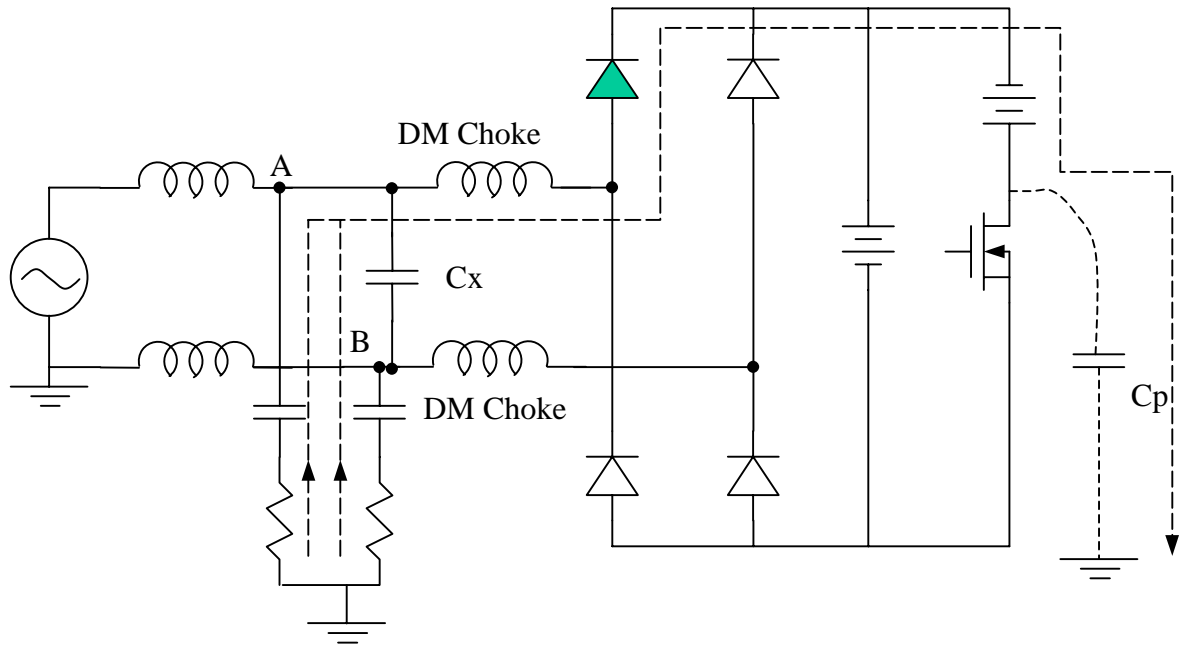


(b) Rectifier Diodes Off, MOSFET Turned Off (C_p Charged)

Fig.3-16 Noise Path Model with X Cap on EUT Side



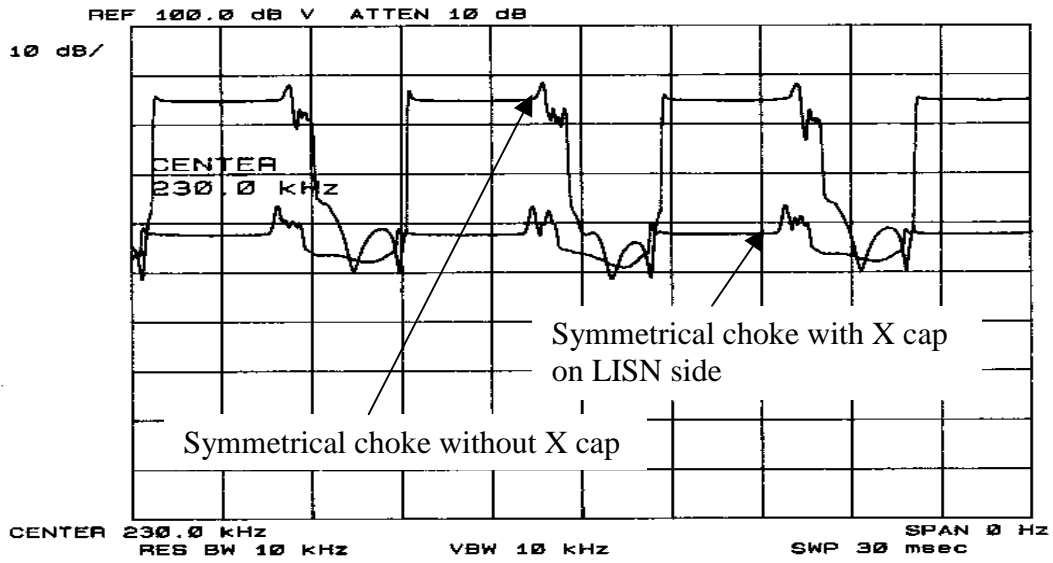
(a) Rectifier Diodes Off, MOSFET Turned On (C_p Discharged)



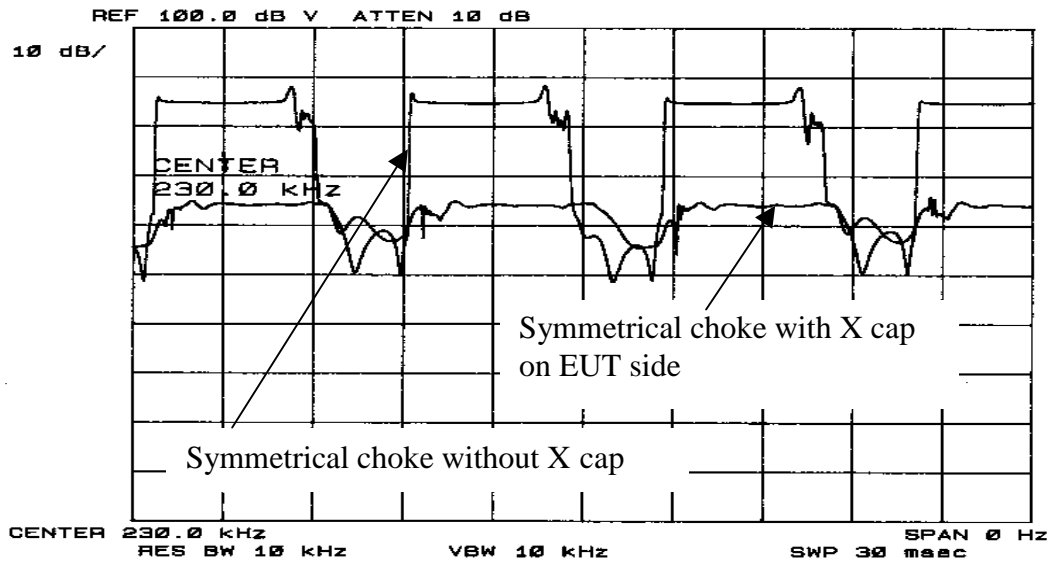
(b) Rectifier Diodes Off, MOSFET Turned Off (C_p Charged)

Fig.3-17 Noise Path Model with X Cap on LISN Side

From the noise path models, it is clear that if the filter topology is symmetrical, the X capacitor will have same effect no matter whether it is placed on the LISN side or the EUT side. Because in either case, there are balanced currents through the two LISN resistors during C_p charging and discharging, the NIDM noise is reduced by large amount. This conclusion can be verified by the following experimental results, which are shown in Fig.3-18.



(a) X Cap on LISN Side



(b) X Cap on EUT Side

Fig.3-18 DM Noise with Symmetrical Choke and X Cap

3.4 Effect of CM Chokes on NIDM

Conventionally, theory says that CM choke has no suppressing effect on DM noise except that the leakage inductance of the CM choke should have some effect on DM noise. This is true, however, only for IDM. For NIDM, CM should have suppressing effect when the two paths are unbalanced, i.e. without a balancing capacitor C_x . Fig.3-19 shows the experimental setup.

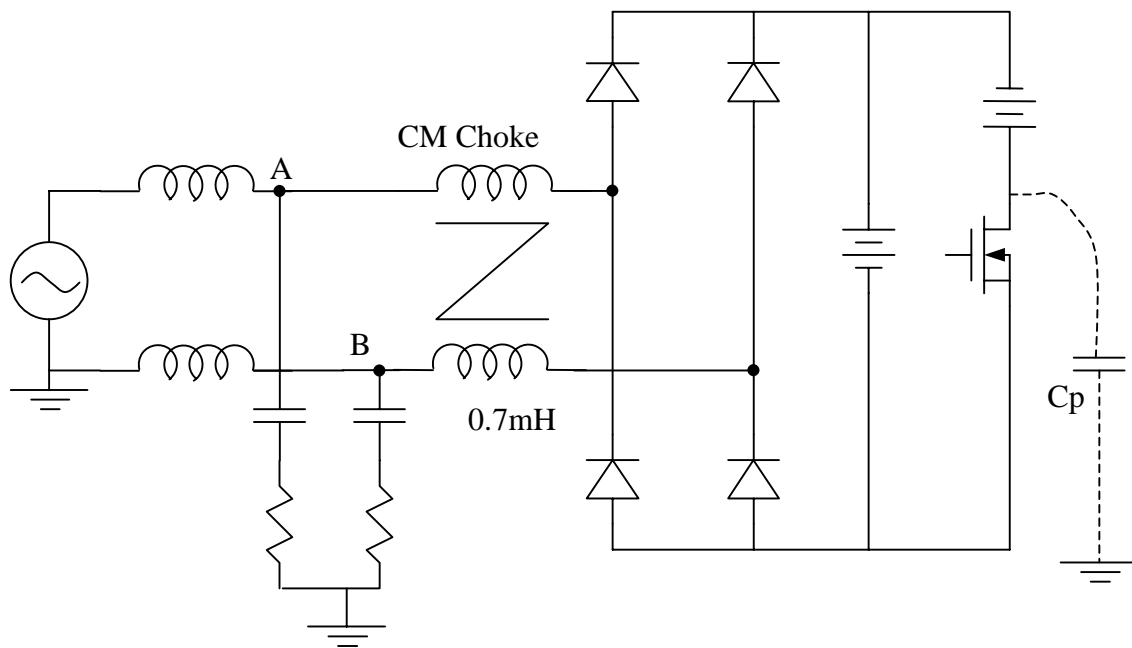


Fig.3-19 Experiment Setup for CM Choke Effect

Fig.3-20 shows the effect. Notice that for IDM portion (interval B), the suppression due to CM choke is minor, which supports conventional EMI theory. However, the attenuation of the NIDM portion (interval A) is very pronounced. Even though noise current is unbalanced as shown in Fig.3-19, but the magnitude of both currents are attenuated already by the CM choke whether D1 or D3 conducting and therefore, the NIDM noise is small. Since CM choke is normally much larger than DM choke in inductance, therefore, CM choke can suppress the NIDM noise effectively also. Fig.3-19 shows the total DM noise attenuation.

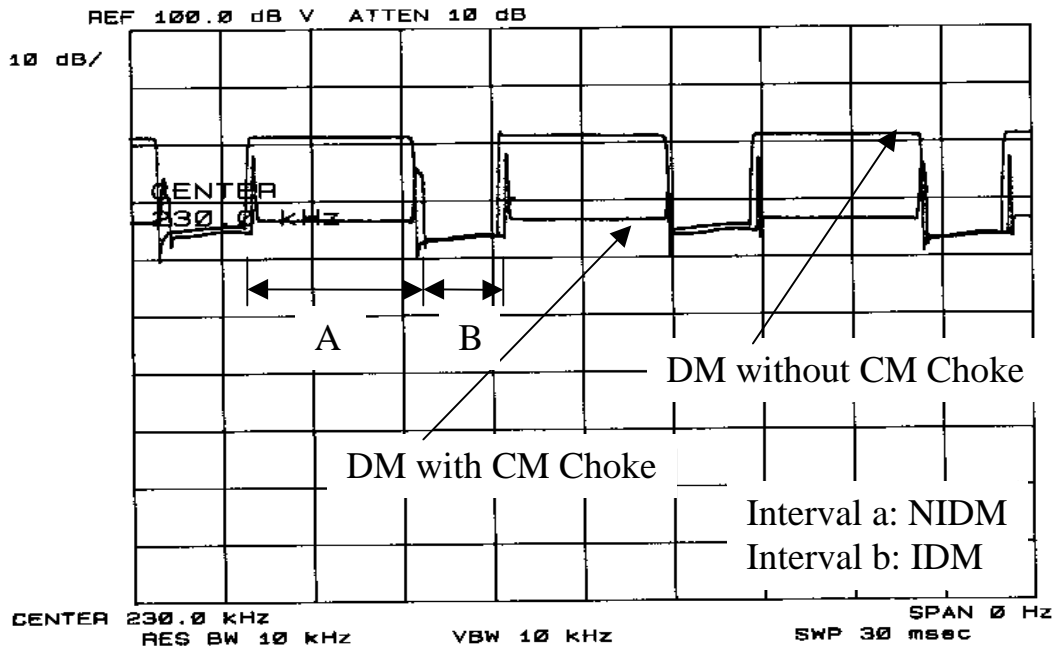
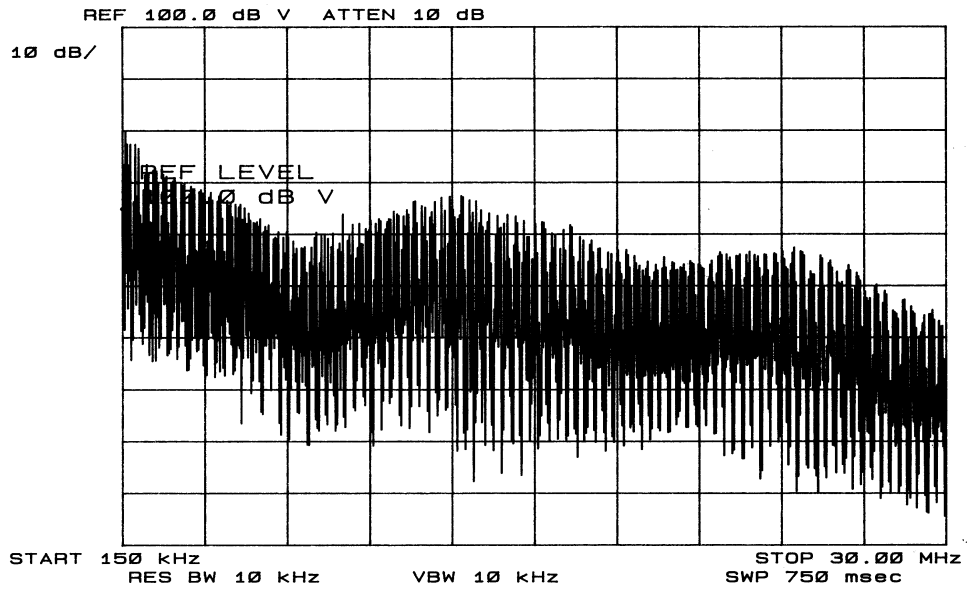
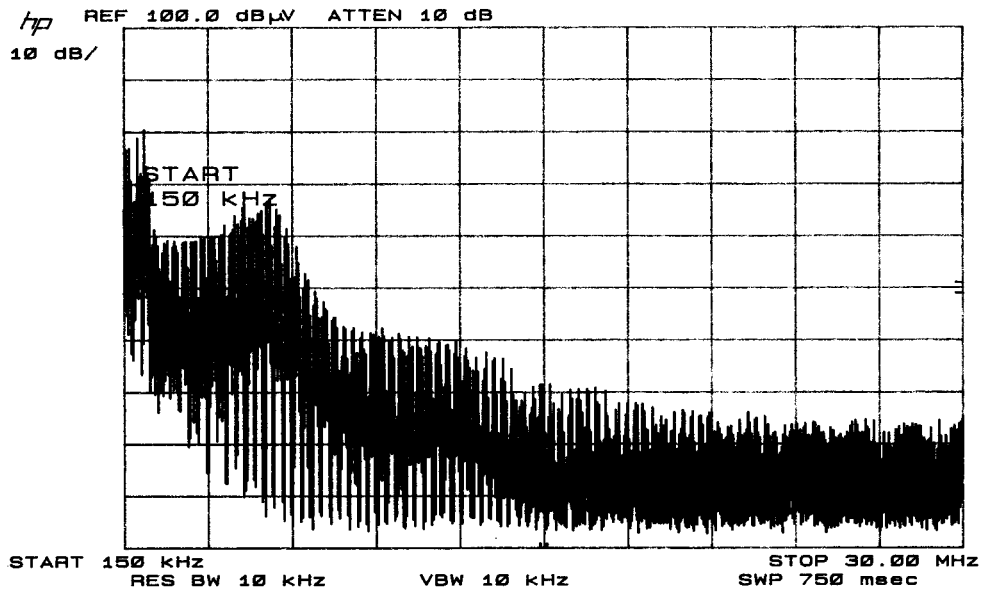


Fig.3-20 Effect of CM Choke on NIDM (Zero-Span Mode)

Fig.3-21 shows the comparison of total DM noise spectrum with and without CM choke.



(a) Without CM Choke



(b) With 0.7mH CM Choke

Fig.3-21 Effect of CM Choke on DM Noise

3.5 Determination of Balancing Cap (X Cap) Value

To effectively suppress the NIDM noise, the balancing capacitor should provide balanced impedance such that the currents flowing through the two LISN resistors R1 and R2 are about the same whether Cp is charged or discharged. Under this condition, the choice of Cx value depends on frequency and the filter topology. The discussion is given below.

(A) When Cx is placed on the LISN side as shown in Fig3-22, then the condition is

$$\frac{1}{2\pi f C_x} \ll 50 \Omega \quad (1)$$

Where f is the start frequency of EMI noise specs (150 kHz for VDE and 450 kHz for FCC). As long as the Eq. (1) holds, the two current paths are balanced. This is true whether there is DM choke or CM choke in the filter.

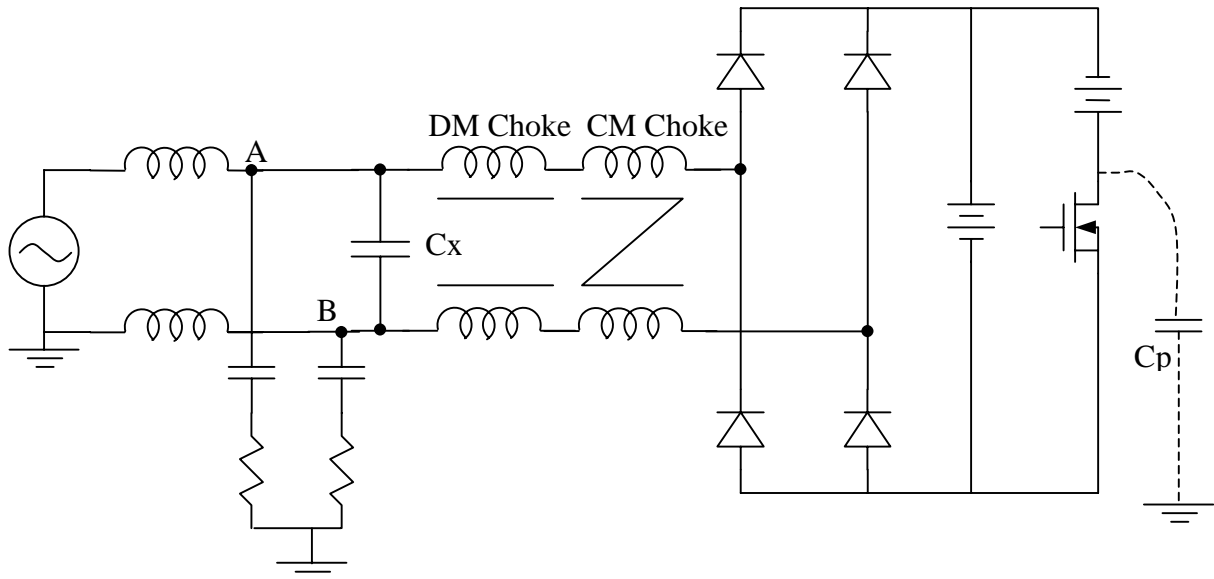


Fig.3-22 X Capacitor on LISN Side

(B) When C_x is on the EUT side as shown in Fig3-23, the condition is

$$\frac{1}{2\pi f C_x} \ll |50 + j2\pi f (L_D + L_C)| \quad (2)$$

Where L_D is the DM choke inductance of each line and L_C is the CM choke inductance.

As explained in Section 3.3, using symmetrical choke L_D on both lines is effective. From Eq. (1) and (2), it can be seen that C_x can be much smaller, if C_x is placed on the EUT side when chokes are used in the filter.

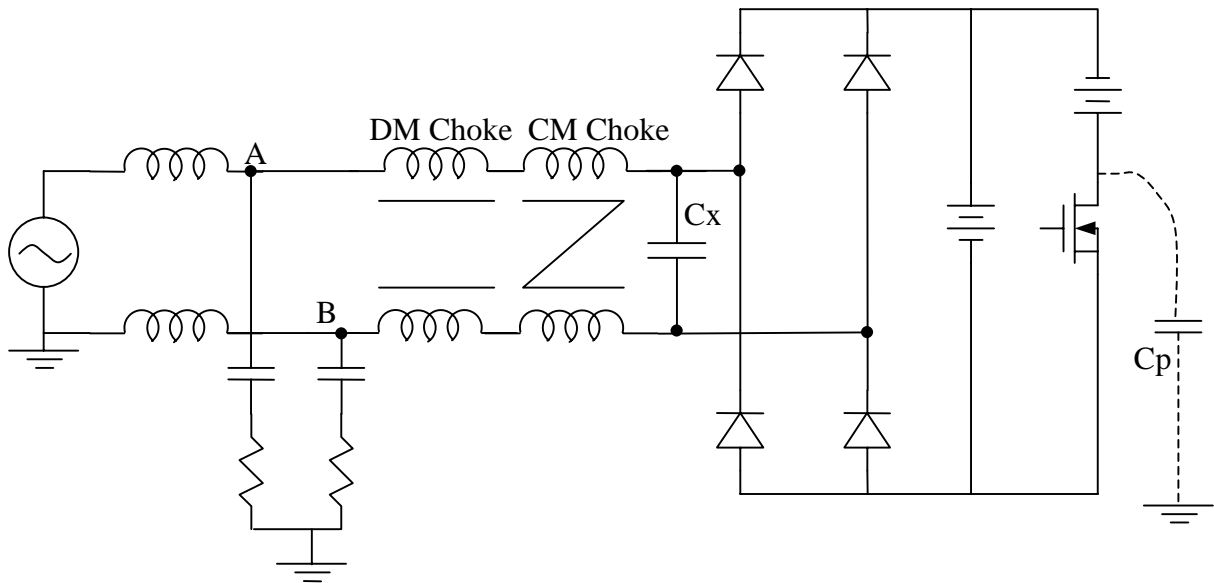


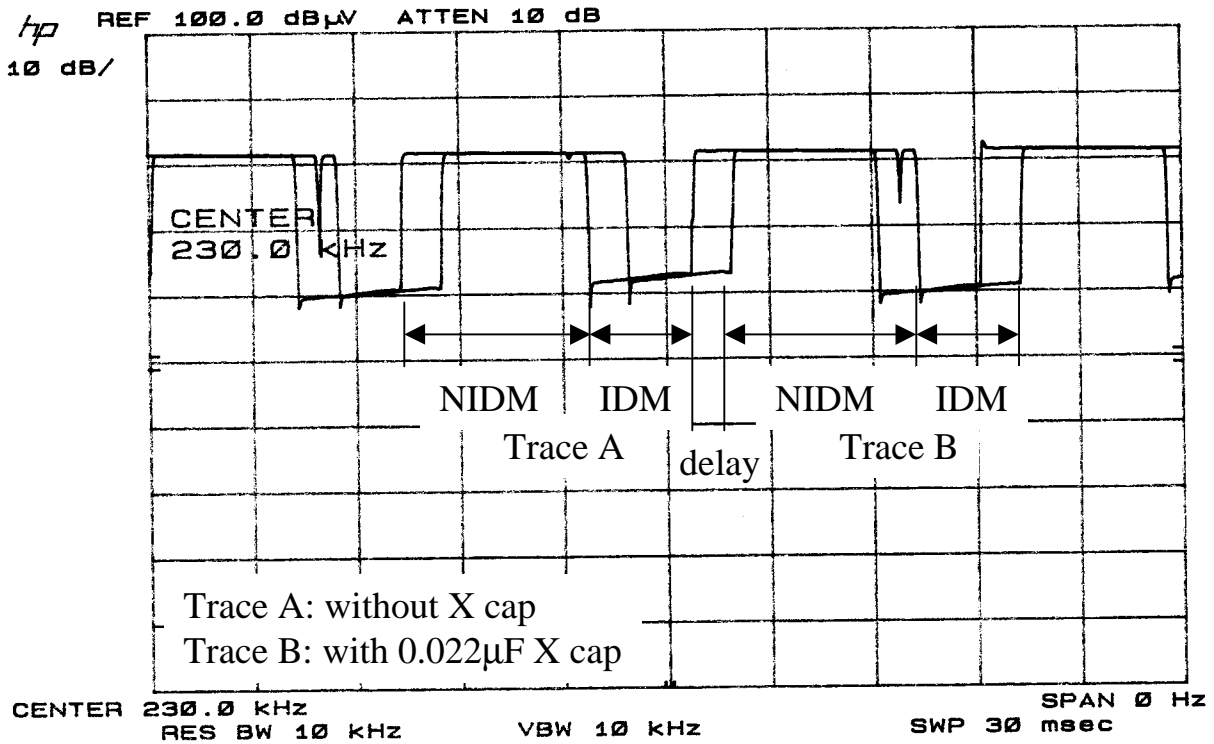
Fig.3-23 X Capacitor on EUT Side

Fig.3-24 (a) shows the NIDM suppressing effect when a 0.022μF X capacitor is used:

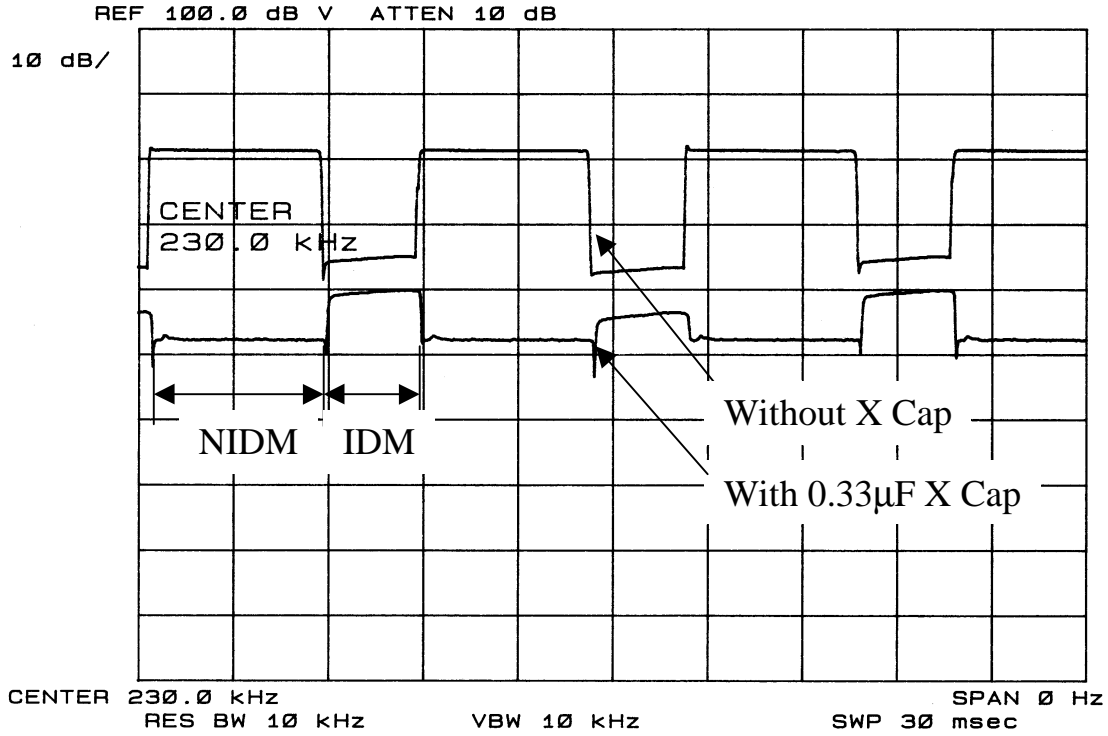
$$\frac{1}{2\pi f C_x} = \frac{1}{6.28 \times 150 \times 10^3 \times 0.022 \times 10^{-6}} \cong 50 \Omega$$

And Fig.3-24 (b) for the case when a 0.33μF X capacitor is used:

$$\frac{1}{2\pi f C_x} = \frac{1}{6.28 \times 150 \times 10^3 \times 0.33 \times 10^{-6}} \cong \frac{1}{10} \times 50 \Omega$$



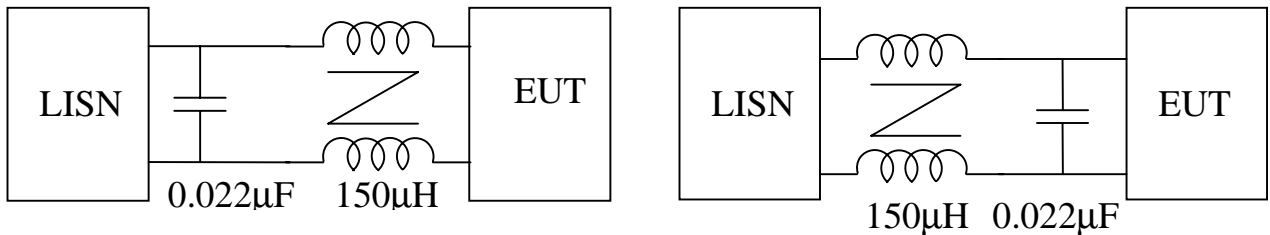
(a) DM with 0.022μF X Cap on LISN Side
(Trace B is delayed purposely for a better view)



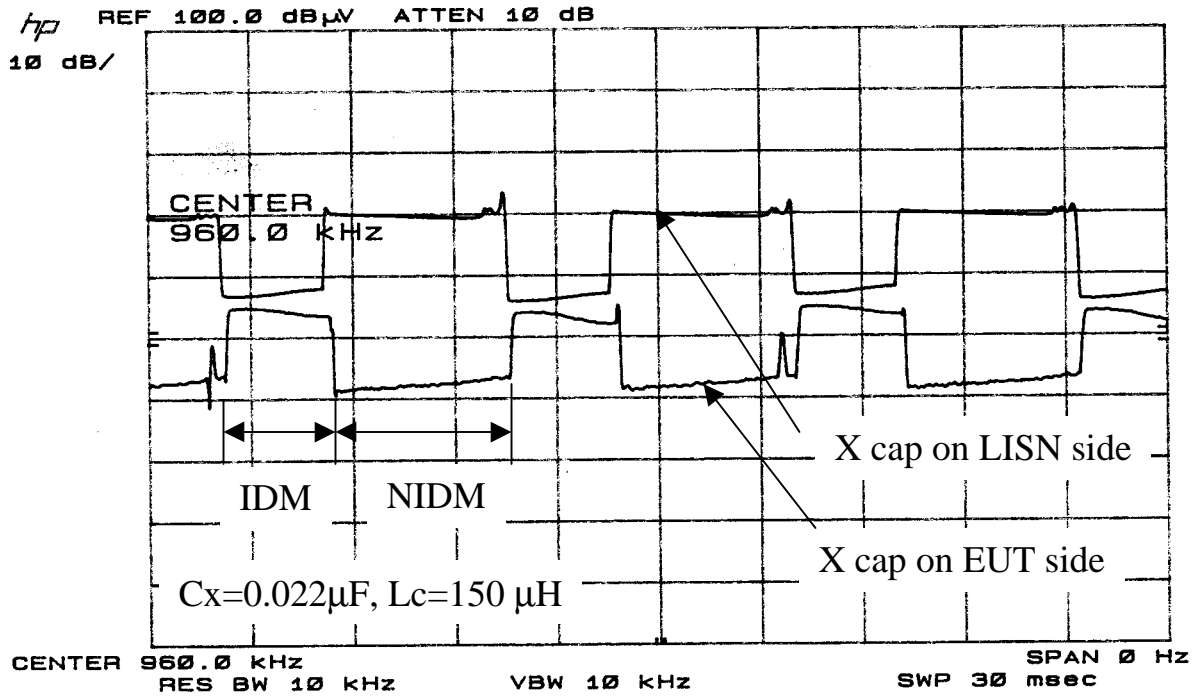
(b) DM with 0.33µF X Cap on LISN Side

Fig.3-24 Impedance of X Cap Affects NIDM Attenuation

Fig.3-25 confirms that when C_x on the EUT side is more effective in the case when DM chokes or CM chokes are placed in the filters. The inductance of the CM choke is 150µH in the following example.



(a) Experimental Configuration



(b) Experimental Result

Fig.3-25 Same X Cap on LISN Side or EUT Side

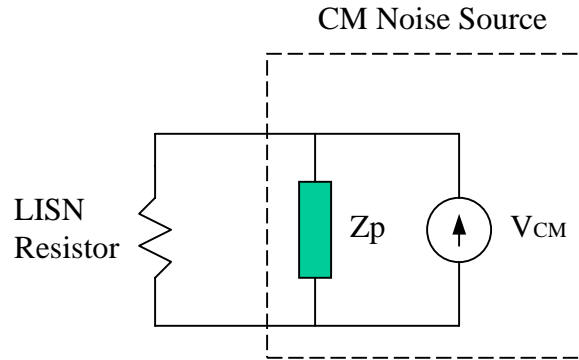
Chapter 4 EMI Filter Design Incorporating NIDM

4.1 Basis for EMI Filter Design

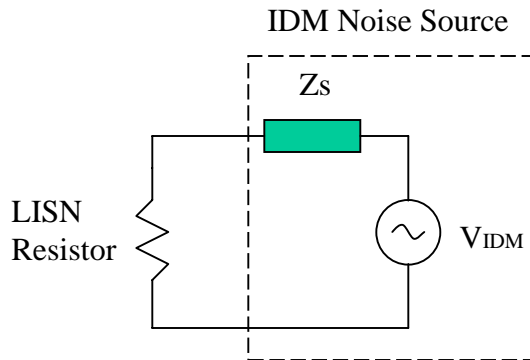
In view of the NIDM phenomenon described in Chapter 3, the conventional filter design procedure needs modification. The end result of the modification is smaller differential-mode filter. A design example will be given and verified in this chapter.

4.1.1 Noise Source Impedance

Because NIDM noise can be suppressed by CM choke and balancing capacitor, the main concern in EMI filter design is CM and IDM noise. The equivalent circuit model of CM noise source is a current source with high parallel impedance, and the model of IDM source is a voltage source with low series impedance as shown in Fig.4-1 (a) and (b) respectively.



(a) CM Noise Source



(b) IDM Noise Source

Fig.4-1 Equivalent Model of Noise Sources

4.1.2 Possible Filter Topologies

Based on the characteristics of noise source impedance, the effective filter component arrangement can be found. Only first and second order filters are discussed in this section. The filter topologies of higher orders are beyond the scope of this thesis.

For noise sources of high impedance, such as CM source, the effective way of attenuation is to use a low impedance element in parallel with the noise source. Because capacitors can provide low impedance at high frequency, the single capacitor filter is the most effective first-order topology for CM noise source. Sometimes, an additional filter element is used to increase the impedance mismatch. That element should provide high impedance in series with the load. Because inductors have high impedance at high frequency, the inductor-capacitor topology with the capacitor adjacent to the noise source is the most effective second-order filter for CM. That topology is called LC filter in this thesis. The topologies are shown in Fig.4-2.

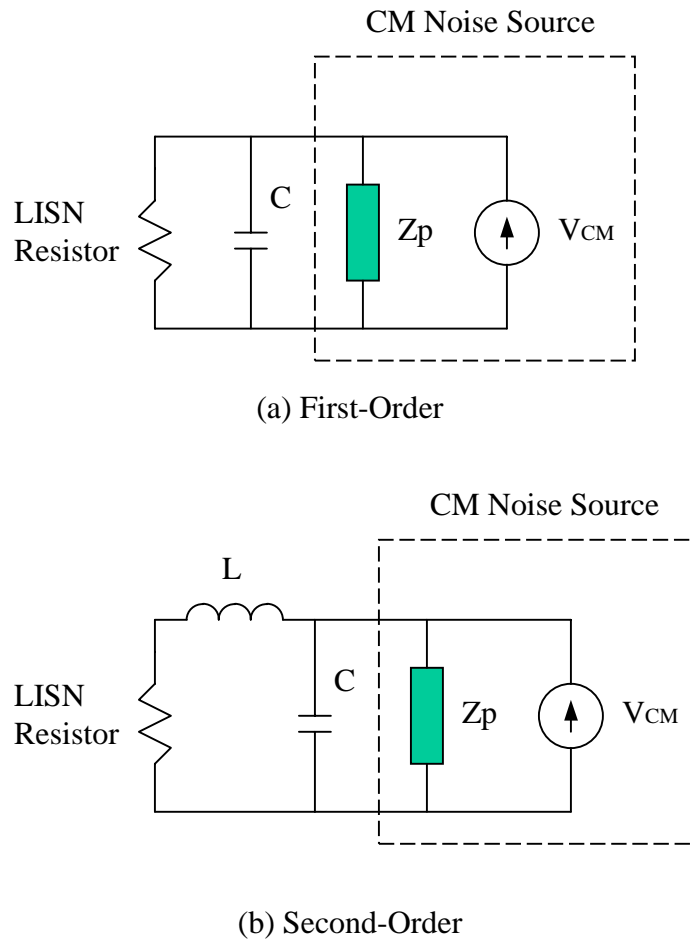


Fig.4-2 Effective Filter Topologies for CM Noise

For noise sources of low impedance, such as IDM source, the effective way of attenuation is to use a high impedance element series with the noise source. The single inductor filter is the most effective first-order topology for IDM noise source. For second-order topology, the additional element should provide low impedance in parallel with the load. The inductor-capacitor topology with the inductor adjacent to the noise source is the most effective second-order filter for IDM. That topology is called CL filter to distinguish it from the one used for CM source. The topologies are shown in Fig.4-3.

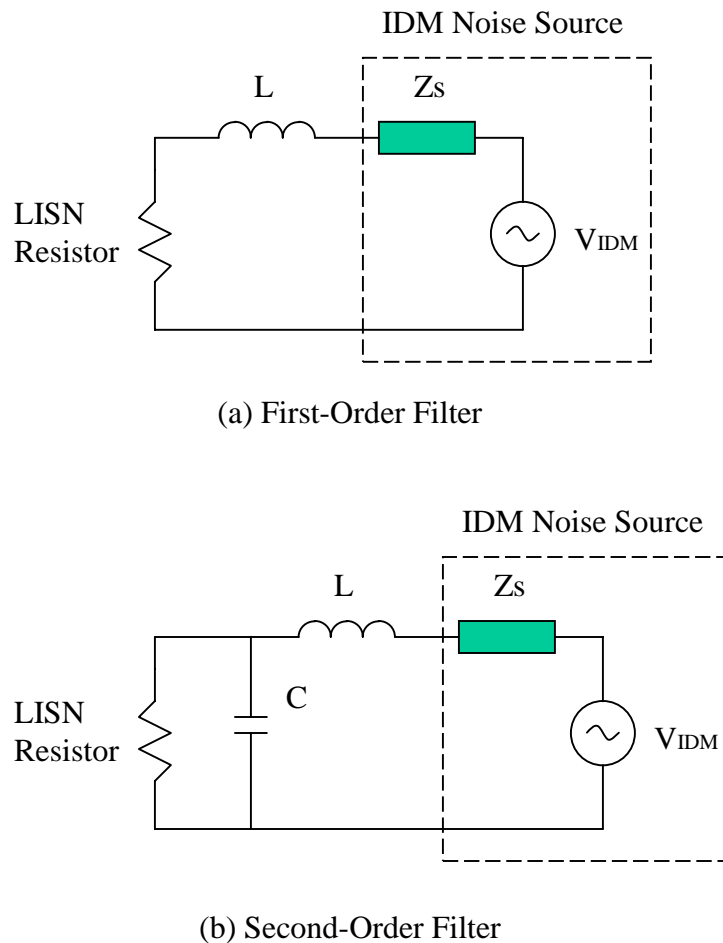
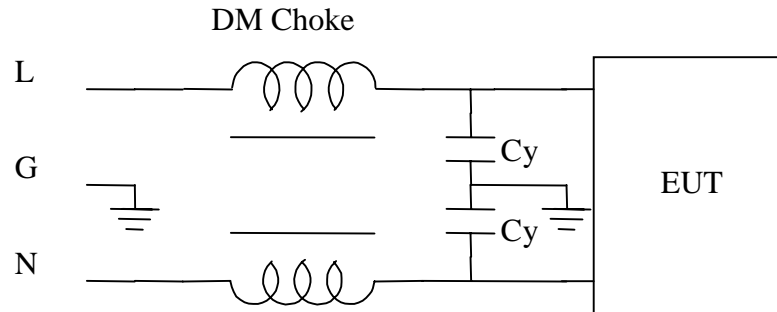
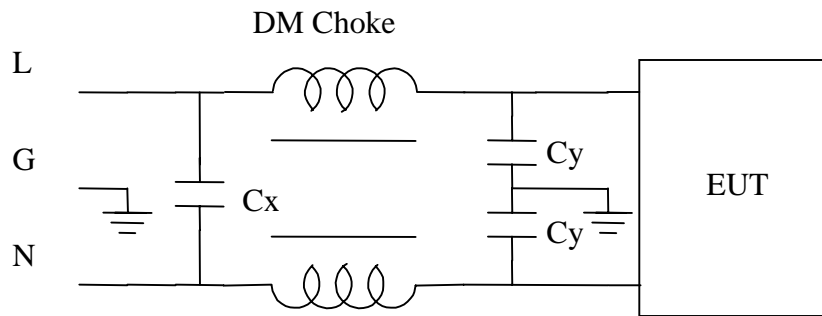


Fig.4-3 Effective Topologies for IDM Source

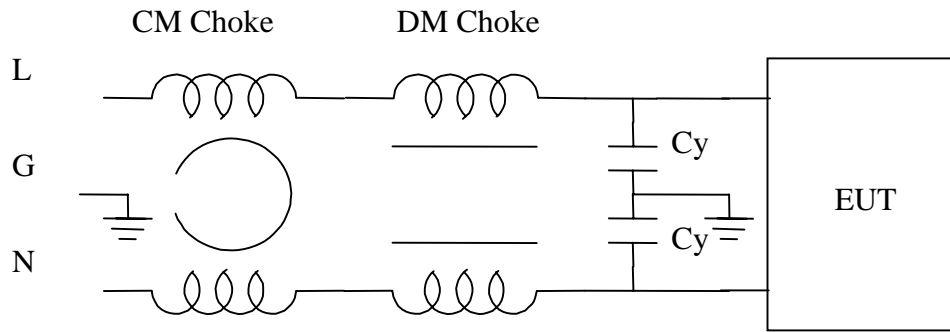
The complete EMI filter is the combination of CM section and DM section. There are four available topologies, which comply with the above arrangement rules. Fig.4-4 shows these four filters.



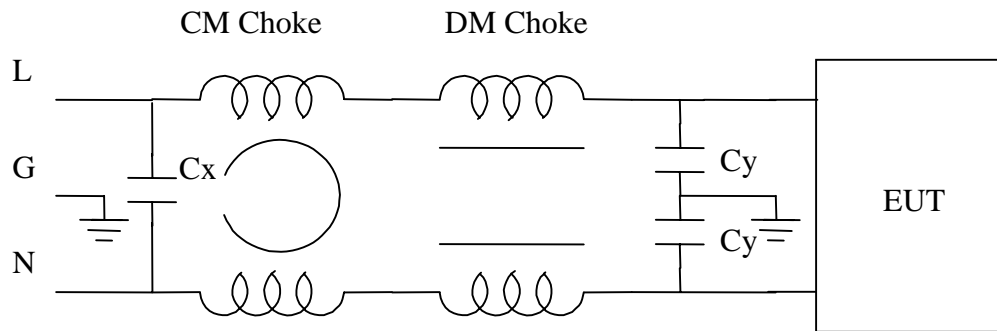
(a) First-Order CM and First-Order DM



(b) First-Order CM and Second-Order DM



(c) Second-Order CM and First-Order DM



(d) Second-Order CM and Second-Order DM

Fig.4-4 Available EMI Filter Topologies

4.2 Determine the Position of X Capacitor

According to the discussion in Section 4.2, the X capacitor will be more effective if it is placed on the LISN side because of the low source impedance of IDM noise source. But if NIDM is considered and symmetrical filter topology being used, X cap on the EUT side is a better choice. Fig.4-5 summarizes the comparison result.

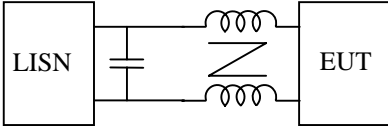
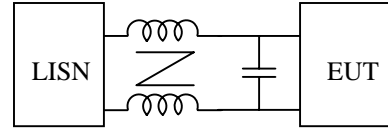
	IDM	NIDM
	More Effective	Less Effective
	Less Effective	More Effective

Fig.4-5 Comparison of X Cap on LISN Side and on EUT Side

When determining the position of X cap, several issues need to be considered simultaneously. If asymmetrical filter topology is being used, then the X capacitor should always be placed on the LISN side. If symmetrical filter topology is used, the position of X capacitor will depend on the DM noise components. If IDM is dominant over NIDM, the X capacitor should be placed on the LISN side and if NIDM is dominant, the capacitor should be on the EUT side of the filter.

4.3 EMI Filter Design Procedure

From the previous discussions, it is clear that it is extremely difficult to obtain an EMI filter design analytically. A practical approach was proposed in [3] to deal with the difficult issue. The approach was based on the following three conditions:

- (1) Baseline (i.e. without filter) EMI noise for both CM and DM must be provided.
- (2) If the filter elements are properly arranged and sized, source impedance has little effect. Therefore, analytical design is possible without knowing exactly the source impedance values.
- (3) The focus of the design procedure is to meet the low frequency specification. After the filter is designed and built, high-frequency performance can be tuned if necessary.

The above assumptions lay down the ground for a possible analytical filter design procedure. The flow chart of the design procedure is shown in Fig.4-6. But the method in [3] has its own limitation. In that approach, only one typical filter topology is considered. Although the topology is the most commonly used filter, it cannot be the optimum one for every power supply. So a complete design procedure should be able to consider other filter topologies. Another limitation about that method is that the mechanism and characteristics of NIDM are not being considered in the design procedure.

To overcome these limitations, a new design procedure will be proposed in the present thesis. The new procedure can be regarded as an expansion of the old procedure, because the theoretical bases are the same for both methods.

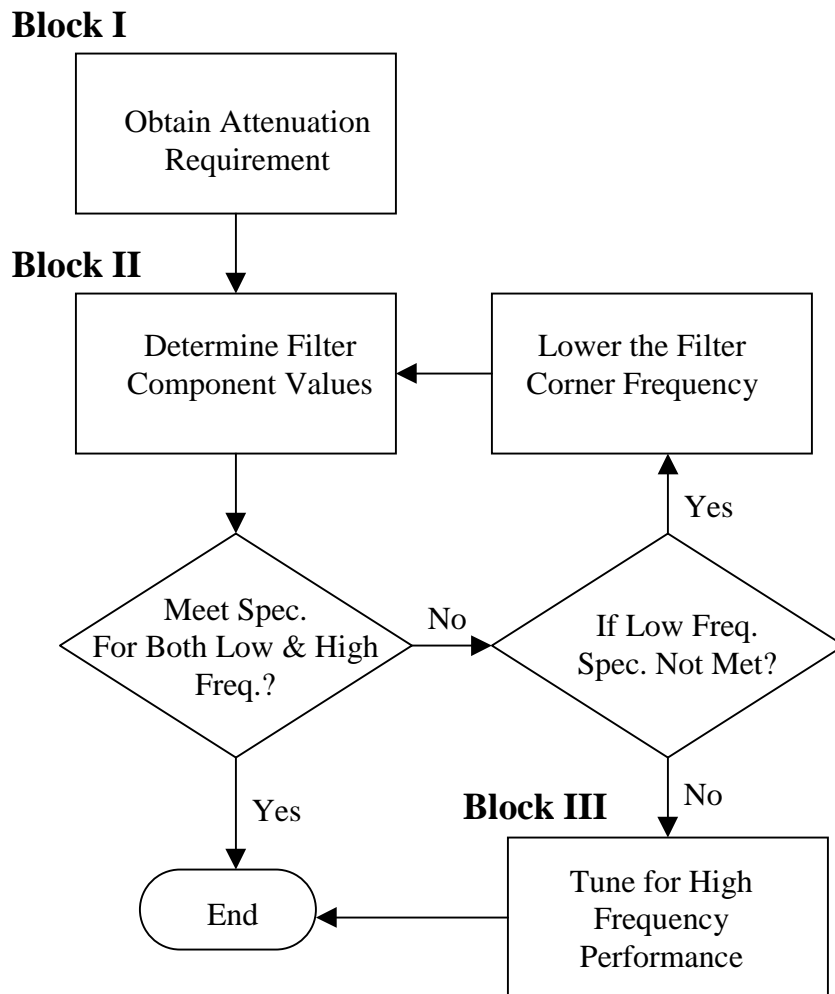


Fig.4-6 Flow Chart for Filter Design

An EMI filter basically consists of two sections: CM section and DM section. These two sections can be designed independently. In Block I of the flow chart, filter attenuation requirements for CM and DM noise are obtained first. This involves the use of noise separator for noise baseline measurement for both CM and DM noise. From

previous discussion, we know balancing noise paths can significantly attenuate NIDM noise. Then the DM section of the filter will solely deal with IDM noise. Therefore, the baseline of IDM noise should be provided. But it is very difficult to separate IDM noise from NIDM noise. One possible solution is to use an X capacitor to balance the noise paths and then measure the DM noise using a noise separator. Because the NIDM has been attenuated by the X capacitor, the remaining DM noise will be IDM. The value of capacitance can be chosen using the method introduced in the previous chapter. Based on the information obtained in Block I, topologies and component values of CM and IDM sections of the EMI filter can be determined in Block II. First, we consider low order filters, such as first-order ones. According to the attenuation curves obtained in Block I, the corner frequency of the filter can be determined. The component values can then be calculated. If the component values are impracticably large, which means filters of higher orders should be used, then we increase the order and recalculate the corner frequency and component values until reasonable component values and attenuation are obtained.

This design is mainly to meet the low frequency specification. Theoretically speaking, the filter design obtained in Block II should meet both the low frequency and high frequency specifications. However, many high frequency effects, which are difficult to predict at the design stage of EMI filters, may cause the violation of design specification at high frequency. Block III provides some possible causes of the high frequency performance degradation, which include high frequency parasitic effects of filter components, permeability roll-off of magnetic material, radiation coupling problems and filter-source impedance interaction.

The design procedure can be summarized into following steps.

Step 1: Measure baseline EMI emission including total noise, CM noise, DM noise and IDM noise. For CM and DM noise measurement, a noise separator is needed. For IDM measurement, an X capacitor is besides the noise separator. The value of the capacitor should be large enough to balance the noise paths.

Step 2: Determine attenuation requirements. The required attenuation is the discrepancy between the baseline noise and the EMI specs plus some correction factor. The correction factor has been discussed previously. It is “+3dB” for CM and IDM attenuation.

$$V_{CM,req} = V_{CM} - V_{spec} + 3dB$$

$$V_{IDM,req} = V_{IDM} - V_{spec} + 3dB$$

Step 3: Choose filter topology. This step also includes determining the order of the filter. Because of the nature of CM and DM noise source impedance, we don't have many choices on topology when the order is determined. All the possible choices have been shown in the Fig.4-4.

Step 4: Determine filter corner frequencies. The attenuation curve of a filter can usually be approximated to a straight line with certain slope when the frequency is beyond the filter corner frequency. The slope is 20dB/decade for first-order filter, 40dB/decade for second-order and 60dB/decade for third-order. To obtain the corner frequency, we can draw such a line and make it tangent to the attenuation curves obtained in Step 2. The horizontal intercept of the line determines the filter corner frequency.

Step 5: Determine filter component values. After determining the filter corner frequency, the filter component values can be calculated using the equations given below.

The derivation of these equations are given in the appendix.

First Order CM Filter

$$f_{R,CM} = \frac{1}{2\pi \cdot 2C_Y \cdot 25} \quad (4-1)$$

Second Order CM Filter

$$f_{R,CM} = \frac{1}{2\pi \cdot \sqrt{L_C \cdot 2C_Y}} \quad (4-2)$$

First Order DM Filter

$$f_{R,IDM} = \frac{100}{2\pi \cdot 2L_D} \quad (4-3)$$

Second Order DM Filter

$$f_{R,IDM} = \frac{1}{2\pi \cdot \sqrt{2 \cdot L_D \cdot C_X}} \quad (4-4)$$

If the calculated component values are impracticably large, filters of higher orders should be considered. Step 3 through Step 5 should be repeated until reasonable filter components are obtained.

Step 6: Check the value of X capacitor. The capacitor in the DM section (on the LISN) also functions as a balancing capacitor. If the capacitor value is not large enough to balance the noise paths, the capacitor needs to be redesigned according to noise path balancing condition discussed in Section 3.5. An alternative is to keep the X capacitor on the LISN side unchanged and to add another capacitor on the EUT side. From the

discussion in Section 3.5, we know a smaller balancing cap is need if it is placed on EUT side.

Step 7: The final step is to measure the noise again with the designed filter. If the low-frequency specs are not satisfied, then the corner frequencies obtained in Step 4 should be lowered and Step 5 should be repeated. If the high-frequency specs are not met, then some tuning measures need to be taken, such as reducing inductor parasitic capacitance, damping undesirable resonance, etc. But that part is beyond the range of this thesis. The design is completed successfully after both low and high frequency parts of the specs can be satisfied.

The complete flow chart of filter design is illustrated in Fig.4-7.

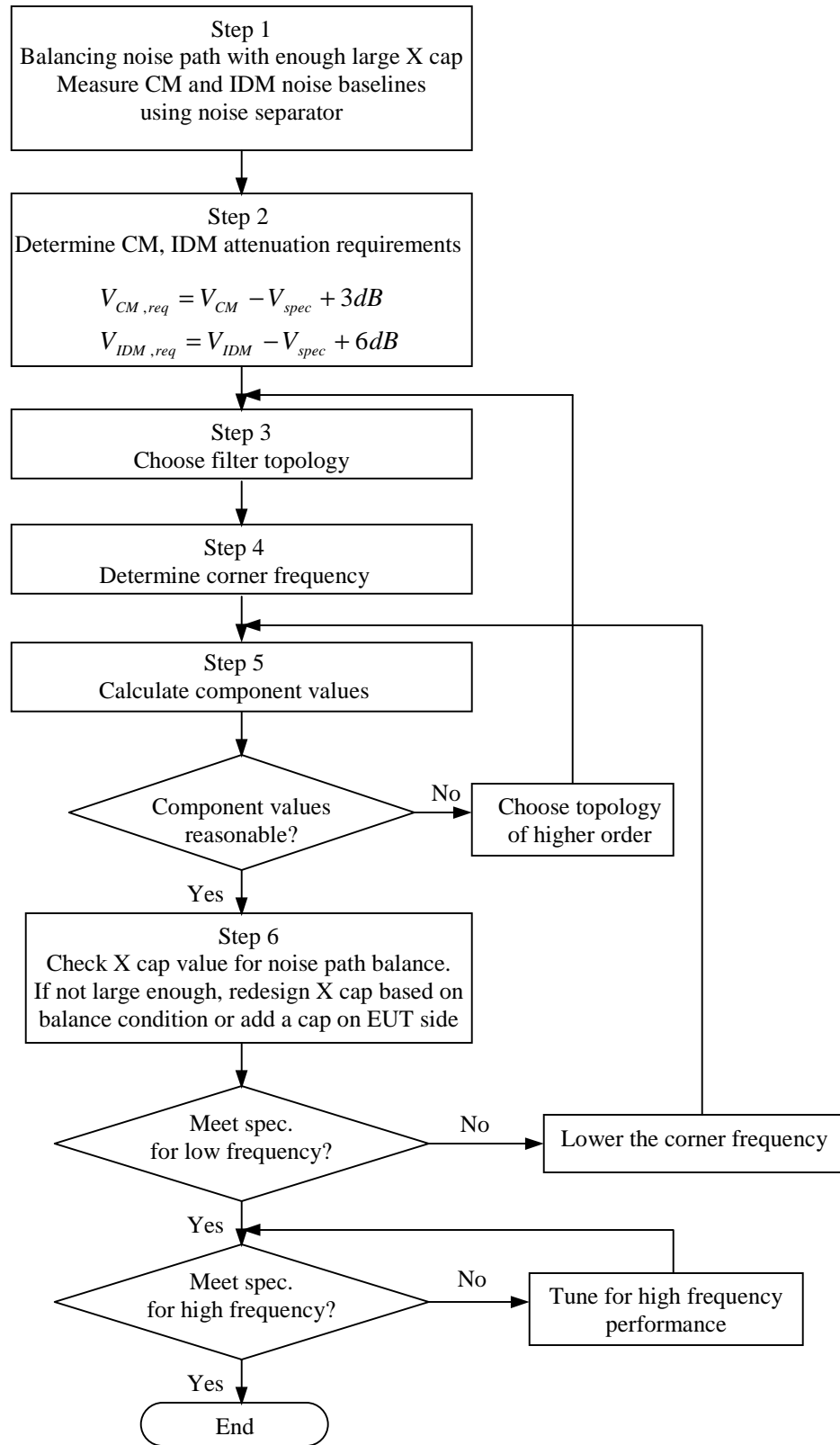


Fig.4-7 Flow Chart of EMI Filter Design

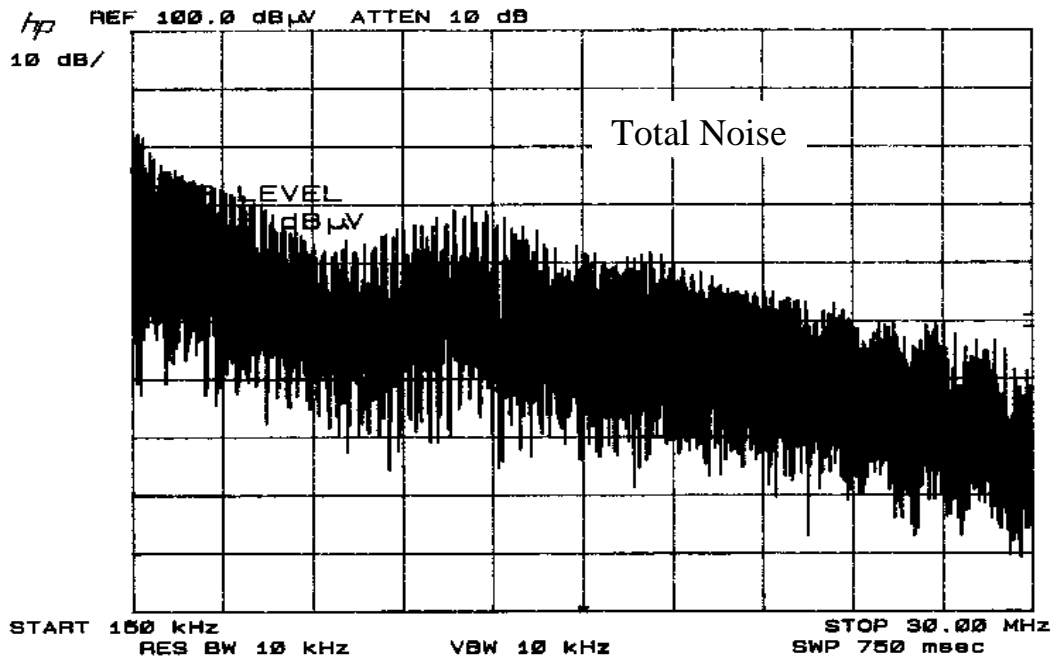
4.4 Design Example

As a design example, the EMI filter for a 100 W flyback offline switching power was design and implemented using the procedure proposed in section 4.2 to meet FCC Class B specification. The input of the power supply is 120 V, 60 Hz single phase AC. The output is 5 V DC. It is noted that the main objective is to meet the low-frequency specs. Once designed and built, modification may be needed to meet the high-frequency specs.

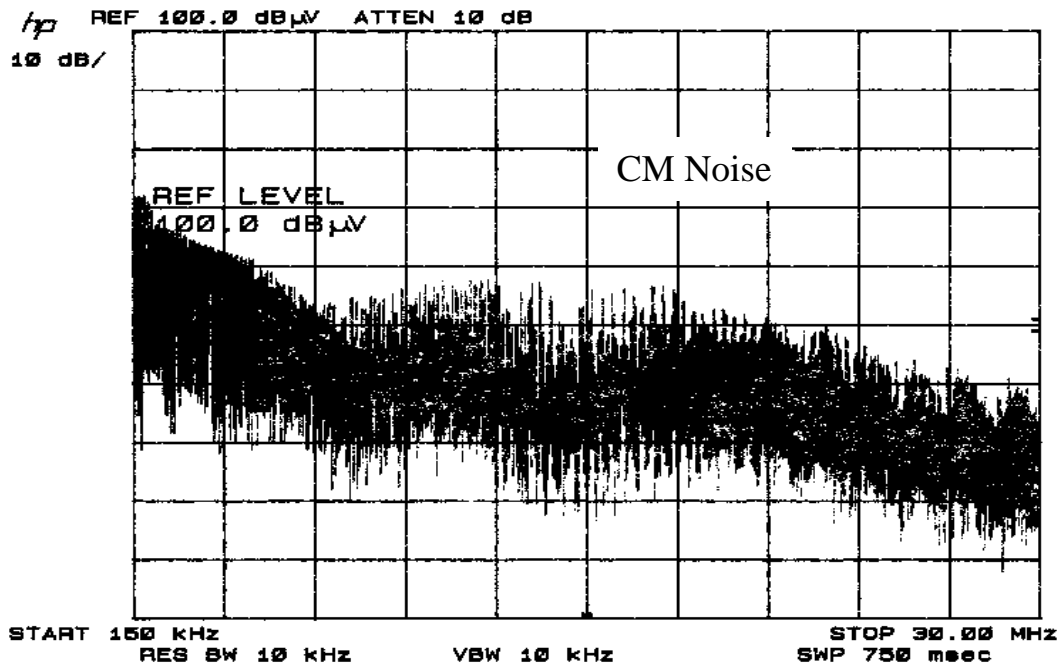
Step1: Measure baseline EMI noise.

First without adding a filter, we measure the total noise, common-mode noise and differential-mode noise respectively. The CM and DM noises can be obtained by using a noise separator. The baseline IDM noise is also needed for filter design. In this example, a 0.47 μ F capacitor (the capacitance was calculated based on the method introduced in Chapter 3) was connected between the phase and neutral lines and then DM noise was measured. Because the capacitor was large enough to balance the noise paths, we can assume the measured DM noise is the same as IDM noise.

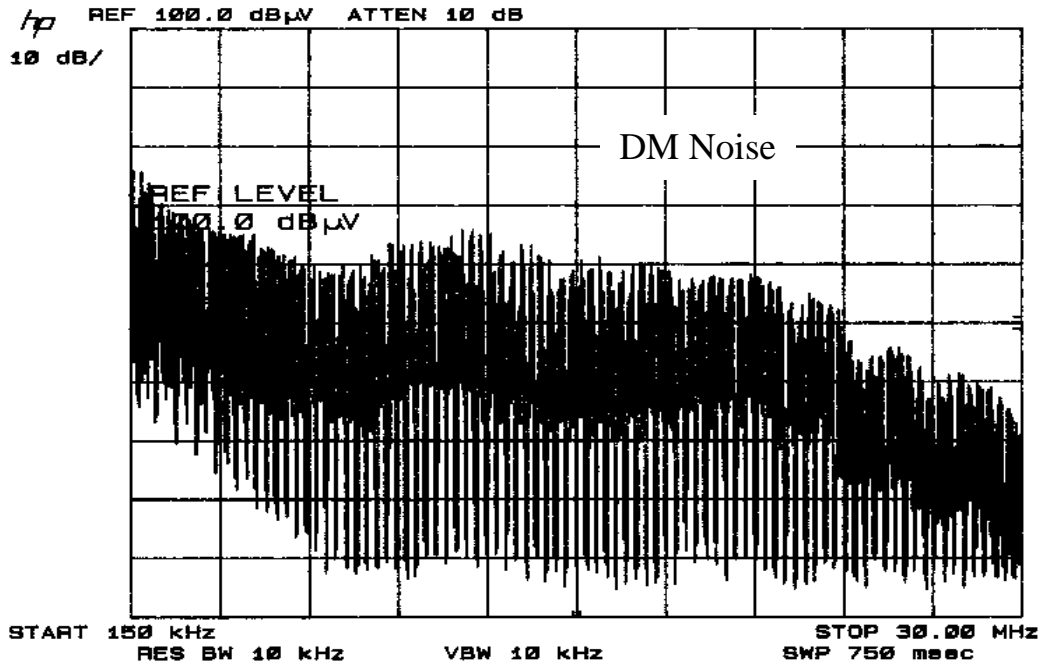
The total noise of the power supply is shown in Fig.4-8 (a), the baseline CM and baseline DM noises are shown in Fig.4-8 (b) and (c). Baseline IDM noise is shown in Fig.4-8 (d).



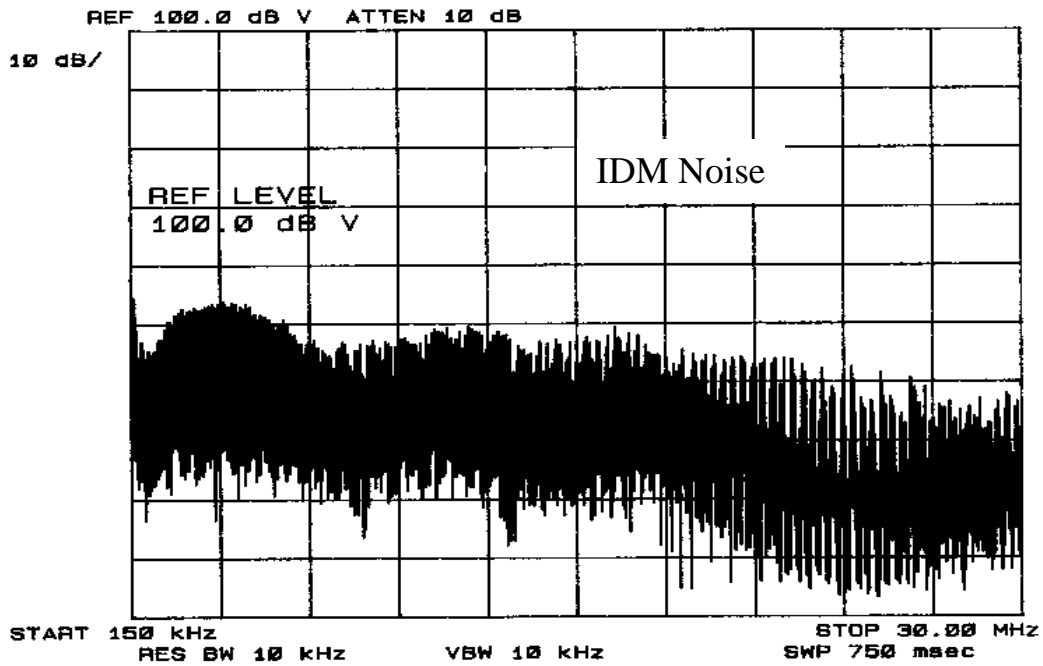
(a) Baseline Total Noise



(b) Baseline Common-Mode Noise



(c) Baseline Differential-Mode Noise



(d) Baseline Intrinsic Differential-Mode Noise

Fig.4-8 Baseline Noise

Step 2 Determine the attenuation requirement

The required CM and IDM attenuation can be calculated from the equations below.

$$V_{CM,req} = V_{CM} - V_{spec} + 3dB$$

$$V_{IDM,req} = V_{IDM} - V_{spec} + 6dB$$

In order to cut down the labor of design work, the design procedure can be implemented in a Mathcad spreadsheet so that the computer can do most of the calculation. It is impossible to put the whole noise spectrum into Mathcad, so some discrete sample points are picked to represent the whole spectrum, especially the low-frequency part. In the example, ten sample points were taken for each noise mode.

Step 3. Choose filter topology

First, we try the simplest filter shown in Fig.4-9. In that topology, CM section is a first-order capacitive filter and DM section is a first-order inductive filter.

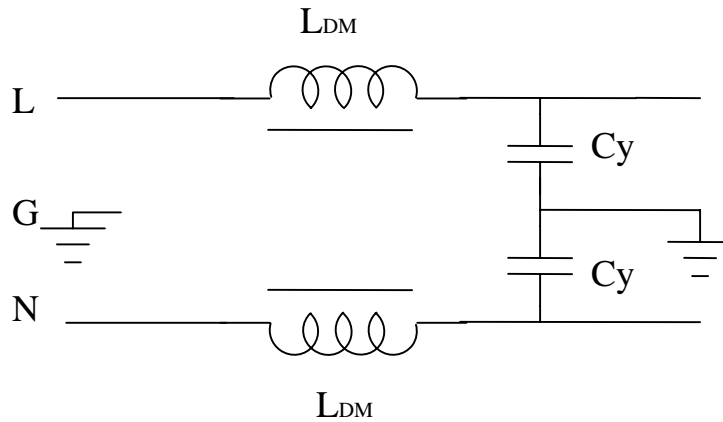
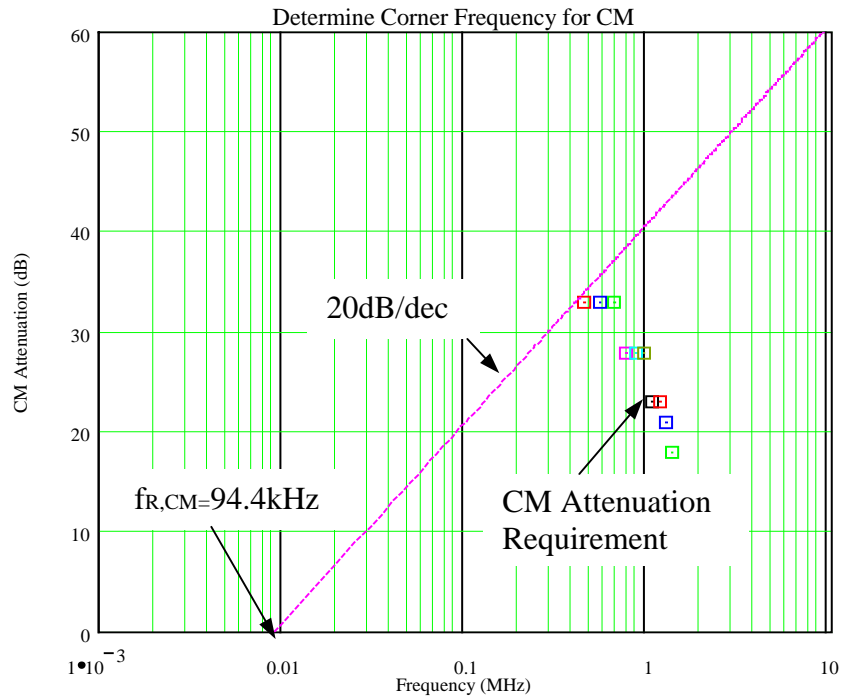


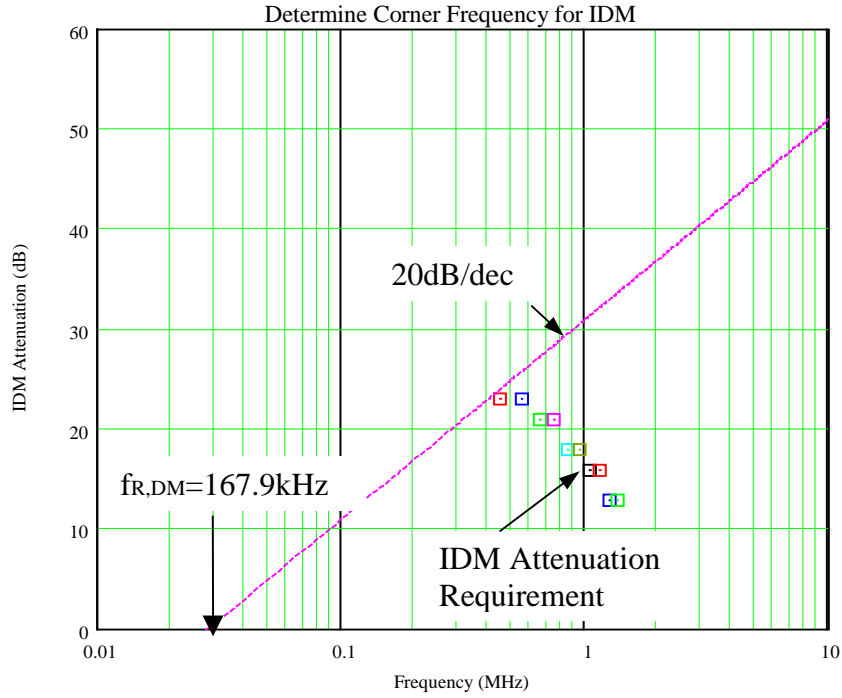
Fig.4-9 First-Order Filter Topology

Step 4. Determine filter corner frequencies

The attenuation curve of a first-order filter can be approximated to a 20dB/decade slope when the frequency is beyond the filter corner frequency.



(a) CM Corner Frequency



(b) DM Corner Frequency

Fig.4-10 Determine Corner Frequencies of First-Order Filter

Step 5. Determine filter component values

(1) Determine CM component values

The only component in the CM section of the filter is C_y , the value of which can be calculated:

$$C_y = \frac{1}{2\pi f_{R,CM} \cdot 50} = \frac{1}{2\pi \times 94.4 \times 10^3 \times 50} = 33.7 \text{ nF}$$

The value of C_y is also determined by the leakage current to the ground. UL requires that current be less than 5mA. Therefore in a 120V, 60Hz power system, the value of C_y

should be less than 4.7nF. The above calculated capacitor value is too high, which means second-order topology should be considered.

(2) Determine DM component values

The only component in DM section of the filter is a symmetrical DM choke. The inductance is given by:

$$2L_{DM} = \frac{100}{2\pi f_{R,DM}} = \frac{100}{2\pi \times 167.9 \times 10^3} = 94.8\mu H$$

The size of the DM choke is reasonable. Because no capacitor is used in a single inductor DM filter, the noise paths cannot be balanced. But in this example, NIDM is dominant in total DM noise, an X capacitor is needed. Therefore, we also should consider second-order topology.

Now we need to repeat step 3 to step 5.

Step 3. Choose filter topology

Now we try another topology with second-order CM and second-order DM sections, which is shown Fig.4-11.

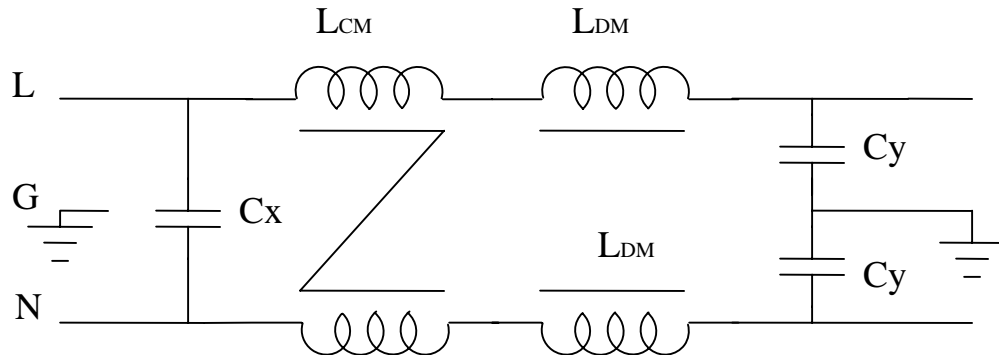
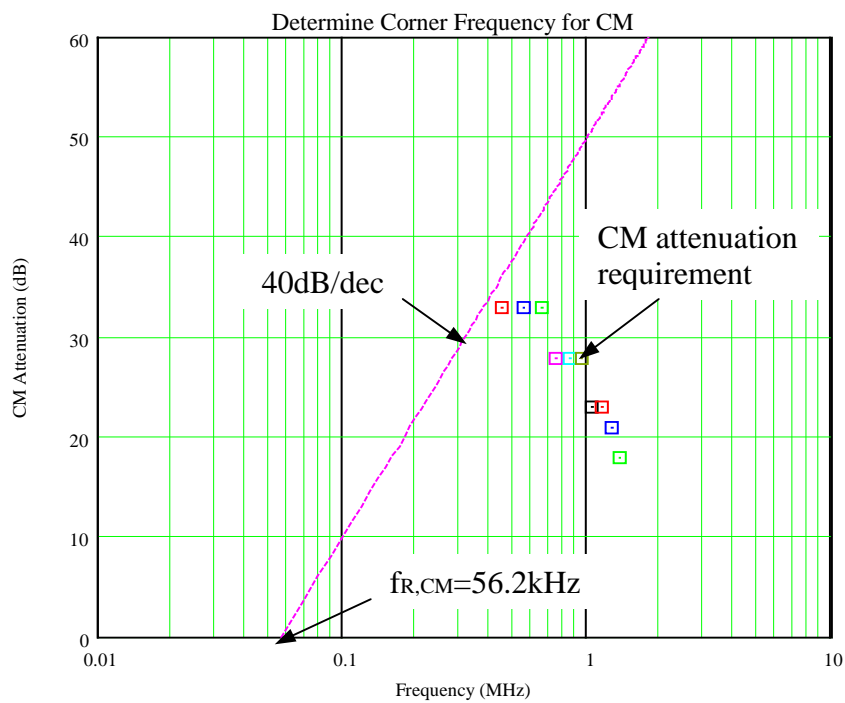


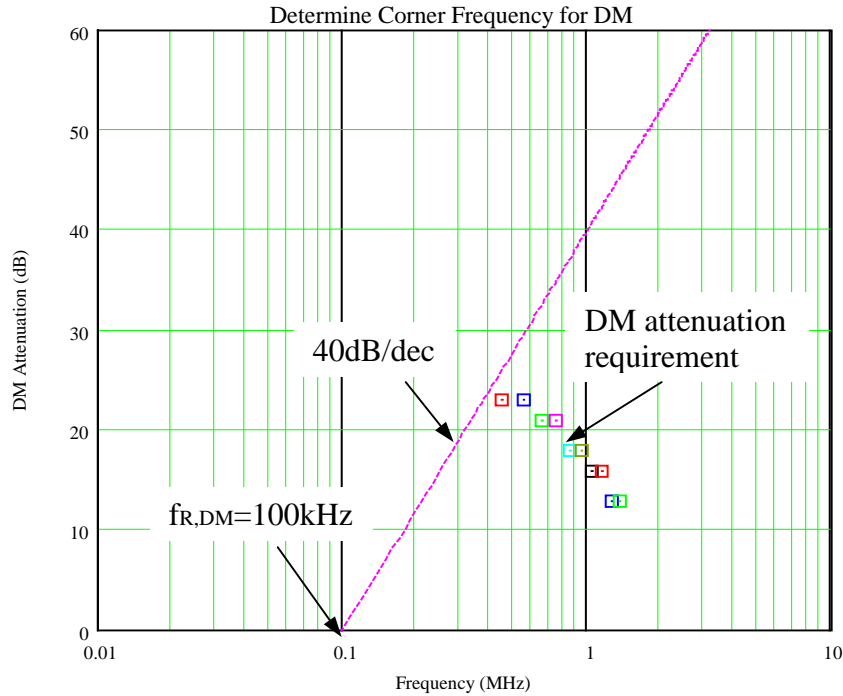
Fig.4-11 Second-Order Filter Topology

Step 4. Determine filter corner frequencies

The attenuation curve of a second-order filter can be approximated to a 40dB/decade slope when the frequency is beyond the filter corner frequency. From Fig.4-12 (a) and Fig.4-12 (b), we can find the corner frequency for CM section of filter is 56.2kHz and for DM section is 100kHz.



(a) Determine Corner Frequency for CM



(b) Determine Corner Frequency for DM

Fig.4-12 Determine Corner Frequencies

Step 5. Determine filter component values

First, the values of CM components are calculated. C_y is determined by the leakage current requirement. We choose:

$$C_y = 4700 \text{ pF}$$

L_{CM} can be calculated according to (4-3)

$$L_{CM} = \left[\frac{1}{2\pi \times 56.2 \times 10^3} \right]^2 \cdot \frac{1}{2 \times 4700 \times 10^{-12}} = 0.85 \text{ mH}$$

We assume the leakage inductance is 2% of the CM inductance

$$L_{leakage} = 17 \mu H$$

The actual leakage inductance can be obtained by measurement.

Then we calculate the values of DM components. As we can see, because the DM section only deals with IDM noise, the attenuation requirement is very low. So we can use the leakage inductance as the DM choke. We have

$$2L_{DM} = L_{leakage} = 17 \mu H$$

Then C_x can be calculated from (4-4)

$$C_x = \left[\frac{1}{2\pi \times 100 \times 10^3} \right]^2 \cdot \frac{1}{17 \times 10^{-6}} = 0.148 \mu F$$

We use the standard value, which is $0.15 \mu F$. The final design values are given in Fig.4-26

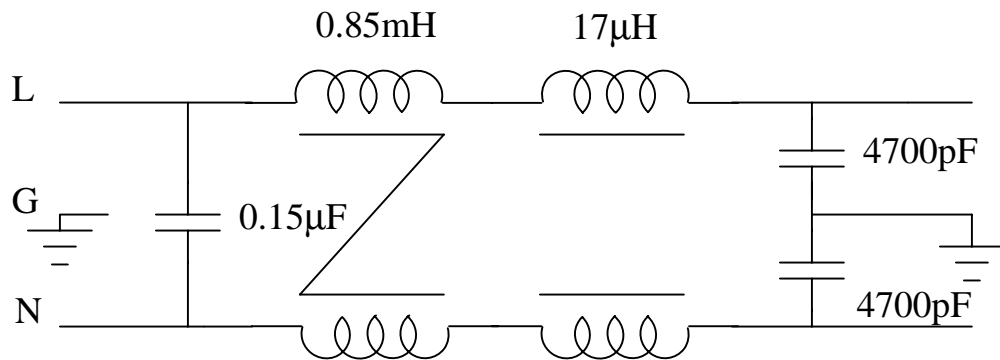


Fig.4-13 Filter Design Values

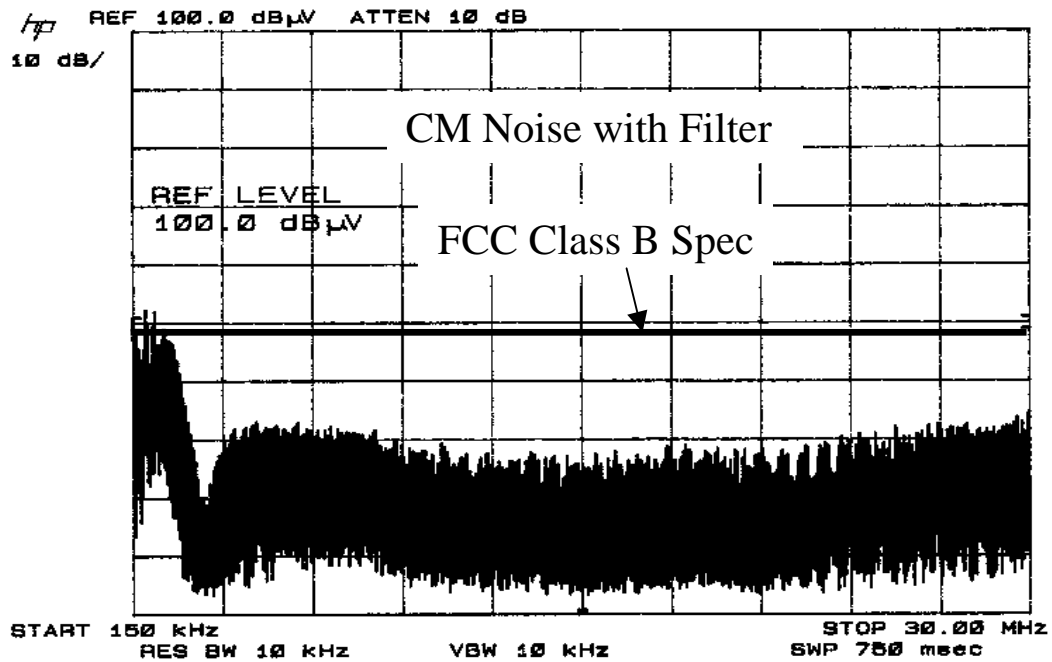
Step 6. Check X capacitor value

The start frequency of FCC specs is 450kHz. The impedance of the capacitor C_x at that frequency is given by:

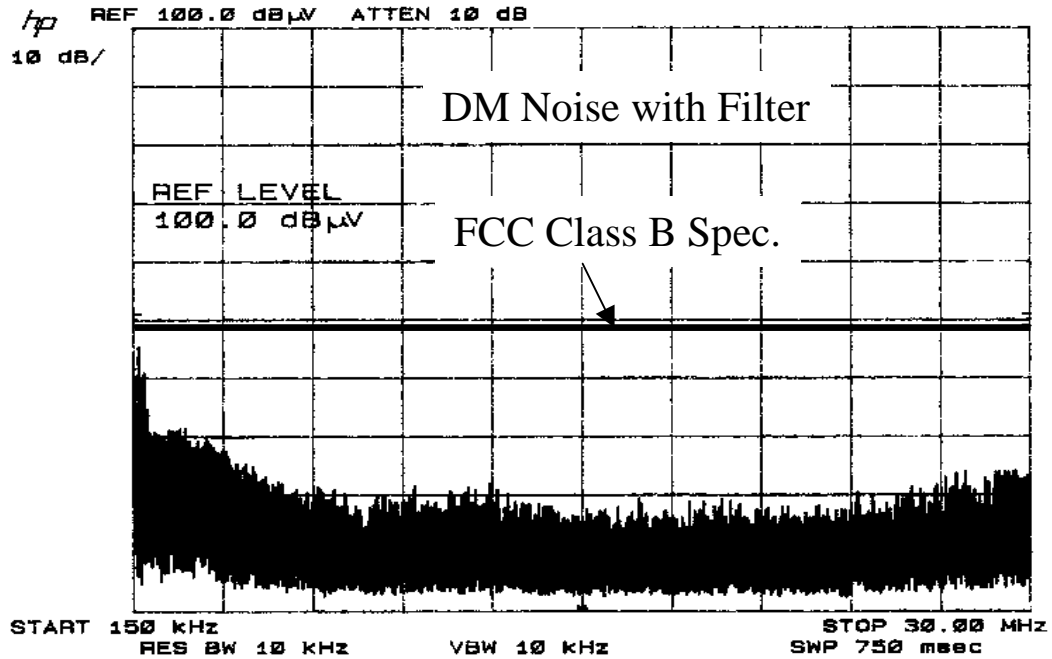
$$\frac{1}{\omega \cdot C_x} = \frac{1}{2\pi f \cdot C_x} = \frac{1}{2\pi \times 450 \times 10^3 \times 0.15 \times 10^{-6}} = 2.36\Omega \ll 50\Omega$$

The value of the capacitor is large enough to balance the noise paths.

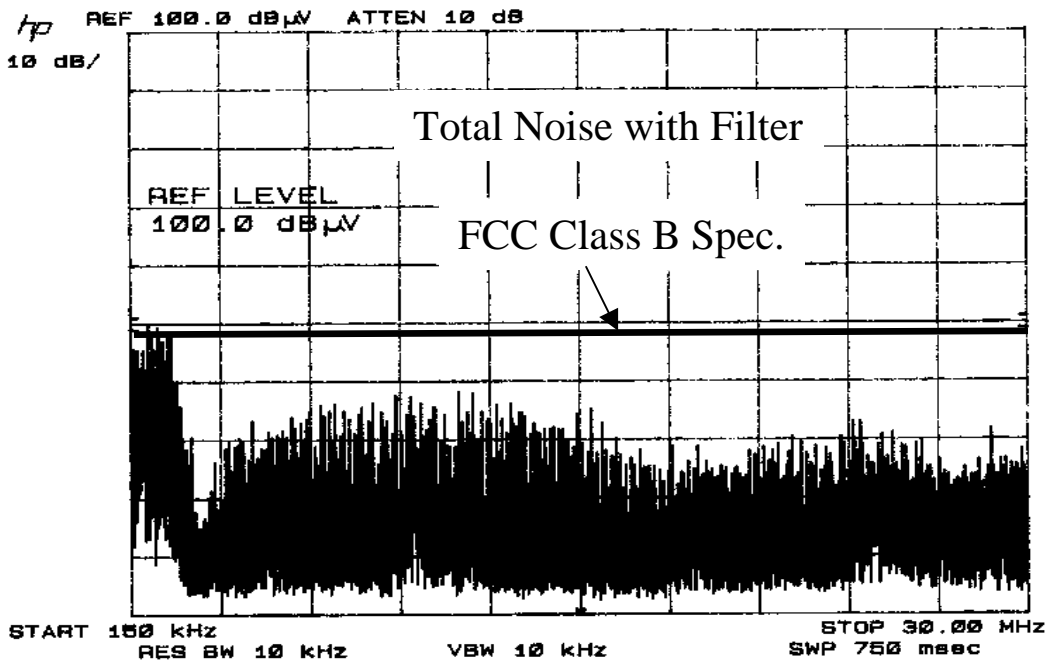
The design is completed. The measurement results are shown in Fig.4-27. We can see the specs have been met.



(a) CM Noise with Filter



(b) DM Noise with Filter



(c) Total Noise with Filter

Fig.4-14 Conducted EMI Emission with Filter

To compare this design procedure with the one proposed in [3], we designed a filter for the same power supply using the old procedure. The design result is shown in Fig.4-15.

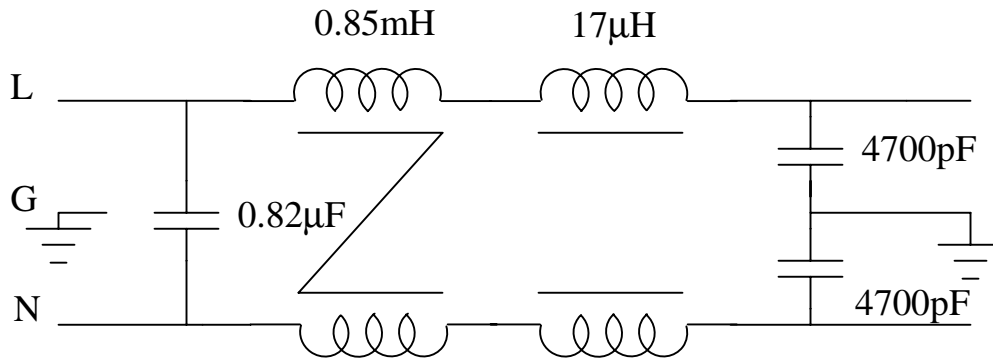


Fig.4-15 Design Result Using Old Procedure

The only difference is that value of the X capacitor in both designs. A 0.82 μF capacitor is used in the filter designed using old procedure. But in the filter designed using new procedure, the capacitor is only 0.15 μF. The difference is caused by the noise baseline measurement. In the new procedure, the IDM noise baseline is measured for the design of DM section of the filter. In many cases, IDM noise baseline is much lower than the total DM noise baseline because of the existence of NIDM. So the old design procedure sometimes can be an over-design if NIDM noise is dominant.

Chapter 5 Conclusions and Future Work

5.1 Conclusions

A new phenomenon, called Non-Intrinsic Differential Mode (NIDM) noise, was investigated and discussed in the thesis. The investigation shows that NIDM noise is a voltage-generated phenomenon. It is related to the charging and discharging of the parasitic capacitance of the MOSFET drain and it couples through the ground path. Therefore, NIDM noise has the nature of CM noise. That feature makes it quite different from the conventional DM noise. But on the other hand, NIDM noise can be detected as DM noise by using a noise separator. Now we know the DM noise is the result of unbalanced noise paths due to the conduction states of the bridge rectifier. Because offline switching power supplies have bridge rectifiers as input stage, the phenomenon of NIDM is very common in this kind of power supplies. Usually the worst case of NIDM is under high line, light load operation condition.

The best way to eliminate NIDM is to balance the noise paths with a capacitor (known as X capacitor) connected between the phase and neutral lines. The capacitor can make the noise current distribute evenly between two LISN branches, but it will not suppress the noise. To reduce the amplitude of the noise, CM chokes should be used. CM choke can effectively attenuate ground noise current, no matter it is in the form of CM or in the form of DM. However, balancing noise paths is still necessary in tackling NIDM.

If the noise currents are unbalanced, the worse case will be considered for CM choke design, which will lead to over-design for the branch with less noise current.

The balance of noise paths depends not only on the conduction of the bridge rectifier, but also on the arrangement of different filter components. Several cases were studied to demonstrate the effect of filter components on NIDM. From the experimental results, we know that symmetrical choke is always better than asymmetrical choke when NIDM is considered. If an inductor-capacitor DM filter topology is used, placing the capacitor on the LISN will be always helpful in eliminating NIDM. But in certain cases, when symmetrical DM chokes or CM chokes are used, the capacitor on the EUT side can also balance the noise paths and smaller capacitance can be used.

The above conclusions can become important guidelines for EMI filter design. A design procedure incorporated with the concept of NIDM was proposed based on an existing one. There are two main differences between the proposed procedure and the existing one. One difference is in baseline EMI measurement. The IDM baseline, instead of DM baseline, is obtained in the new procedure. Another difference is in the design of DM filter. The filter will be designed to meet the IDM attenuation requirement. After the IDM attenuation is met, the noise path balance condition will be checked. If the capacitor in the filter is not large enough to balance the noise paths, some adjustments on the capacitor value will be made or an additional capacitor will be added.

5.2 Future Work

The NIDM investigation in this thesis is limited to single phase offline converters. NIDM phenomenon also exists in three phase converters because of the input bridge rectifier. But that issue has never been studied. The future research will focus on the NIDM phenomenon in three phase offline converters and its implications to EMI filter design.

In the proposed EMI filter design procedures, only first- and second-order filters are considered. Another effort in the future research is to expand the existing procedure to consider third- or higher order filter topologies.

Reference

- [1] Dongbin Zhang, Dan Y. Chen, Mark J. Nave, “Non-Intrinsic Differential Mode Noise Caused by Ground Current in an Offline Power Supply” IEEE PESC Conference Proceedings, Fukuoka Japan, 1998
- [2] Ting Guo, Dan Y. Chen, Fred C. Lee, “Separation of Common-Mode and Differential-Mode Conducted EMI Noise” IEEE Transactions on Power Electronics, Vol. 11, No. 3, May 1996
- [3] Fu-Yuan Shih, Dan Y. Chen, Yan-Pei Wu, Yie-Tone Chen, “A Procedure for Designing EMI Filters for AC Line Applications” IEEE Transactions on Power Electronics, Vol.11, No. 1, January 1996
- [4] Henry W. Ott, “Noise Reduction Techniques in Electronic Systems” John Wiley & Sons, 1988
- [5] Mark J. Nave, “Power Line Filter Design for Switched-Mode Power Supplies” Van Nostrand Reinhold, 1991
- [6] Hewlett Packard, “Operating and Programming Manual: 8568B Spectrum Analyzer” Hewlett Packard Company 1984

Vita:SongQU

The author was born in Tianjin, China. He obtained his BS and MS degrees from Shanghai Jiao Tong University, Shanghai, China in 1993 and 1996 respectively, both in Electrical Engineering.

He was hired as a Project Engineer by Shanghai Sanhuan Electric Control Corporation from January 1996 to June 1997, designing DC and AC drive systems for various industrial applications.

In August 1997, he enrolled at Virginia Polytechnic Institute and State University and started pursuing another Master's degree at Center for Power Electronic Systems (formerly known as Virginia Power Electronics Center). His research interests at C-PES (VPEC) include high-frequency power conversion, analysis of EMI in switching power supplies, emission control and filter design.